Simplified Design Procedures for Moorings of Wave-Energy Converters

Deliverable 2.2

Bergdahl, Lars; Kofoed, Jens Peter

Publication date:
2015

Document Version
Publisher's PDF, also known as Version of record

STRUCTURAL DESIGN OF WAVE ENERGY DEVICES

Simplified Design Procedures for Moorings of Wave-Energy Converters

Lars Bergdahl
Jens Peter Kofoed

Deliverable D2.2

CHALMERS

ISSN 1901-726X
DCE Technical Report No. 172

DEPARTMENT OF CIVIL ENGINEERING
AALBORG UNIVERSITY

Aalborg University
Department of Civil Engineering
Structural Design of Wave Energy Devices

DCE Technical Report No. 172

Simplified Design Procedures for Moorings of Wave-Energy Converters

by

Lars Bergdahl
Jens Peter Kofoed

March 2015

Scientific Publications at the Department of Civil Engineering

Technical Reports are published for timely dissemination of research results and scientific work carried out at the Department of Civil Engineering (DCE) at Aalborg University. This medium allows publication of more detailed explanations and results than typically allowed in scientific journals.

Technical Memoranda are produced to enable the preliminary dissemination of scientific work by the personnel of the DCE where such release is deemed to be appropriate. Documents of this kind may be incomplete or temporary versions of papers—or part of continuing work. This should be kept in mind when references are given to publications of this kind.

Contract Reports are produced to report scientific work carried out under contract. Publications of this kind contain confidential matter and are reserved for the sponsors and the DCE. Therefore, Contract Reports are generally not available for public circulation.

Lecture Notes contain material produced by the lecturers at the DCE for educational purposes. This may be scientific notes, lecture books, example problems or manuals for laboratory work, or computer programs developed at the DCE.

Theses are monograms or collections of papers published to report the scientific work carried out at the DCE to obtain a degree as either PhD or Doctor of Technology. The thesis is publicly available after the defence of the degree.

Latest News is published to enable rapid communication of information about scientific work

Published 2015 by
Aalborg University
Department of Civil Engineering
Sofiendalsvej 11,
DK-9200 Aalborg, Denmark

Printed in Aalborg at Aalborg University

ISSN 1901-726X
DCE Technical Report No. 172

1. Introduction

It would be reasonable that ocean energy devices were designed for the same risk as the platforms in the oil industry. Risk should then be evaluated as a combination of probability of failure and severity of consequences, which means that a larger probability of failure for ocean energy devices would be balanced by the less severe consequences.

The question of some relaxation in safety factors for moorings of wave energy plants has been addressed in the EU Wave Energy Network[i] and at least three times at EWTEC conferences 1995[ii], 2005[iii] and 2013[iv]. Here we will not discuss this but will stick to the present DNV-OS-E301 POSMOOR[v] rules as advised in the Carbon Trust Guidelines[vi].

With ocean energy devices in focus, this report describes comprehensively environmental conditions, environmental loads, and design procedures for moorings.

In this introduction a quasi-static mooring design loop is described, Paragraph 1.2. In Chapter 2 design rules and guidelines are described in relation to design with increased degree of sophistication − from simple quasi-static design to time-domain simulation with coupled dynamic mooring system and free water surface. In Chapter 3 environmental conditions are discussed. Often these are named Metocean conditions ending with a specification of sample design conditions for Hanstholm. In Chapter 4 environmental loads are estimated from the design conditions. We treat loads due to wind, sea currents and waves. The load from sea currents and wind will be treated using almost the same concepts. The wave load is described for individual waves (first-order wave loading) including load from superposed regular wave components in irregular waves, mean wave drift load (second-order wave loading) for regular and irregular waves and slowly varying wave-drift loads. I Chapter 5 the static force-displacement properties of a three-leg Catenary Anchor Leg Mooring System, CALM, is outlined as a basis for the quasi-static mooring design in the end of Chapter 6.

In Chapter 6 for illustrative purposes a quasi-static design of a moored, vertical, cylindrical buoy representative of a point absorber is made, using the Catenary Anchored Leg Mooring described in Chapter 5.

Finally in Chapter 7 the minimum breaking strength of the chosen chain is compared to the design tensions and usage factors for the CALM system with various pretension.

Irregular waves or a sea state is often represented by a spectrum and by multiplication of this, for each frequency, with the linear response ratio in that frequency. For instance, using the motion response ratios a response spectrum of the motion will be produced. Thereafter statistical methods can be utilized to assess characteristics of responses in each sea state or in all anticipated sea states during e.g. 50 years.

For large or steep waves and large relative motions non-linear time-domain or non-linear frequency-domain methods must be used, which is out of scope of this report.

The goal of the report is that the reader shall be able to self-dependently make a first, preliminary analysis of wave-induced horizontal loads, motions and mooring forces for a moored floating wave energy device. Necessary prerequisites to attain that goal are the understanding of the physical phenomena, awareness of simplifying assumptions and some insight into the available mathematical or numerical tools.

1.1 Motions of a Moored Device in Waves

A moored device in waves will be offset by steady current, wind and wave drift and will oscillate in six degrees of freedom. In very long waves its motion will just follow the sea surface motion with some static reaction from the mooring system, but for shorter waves – near the horizontal and vertical resonances of the body-mooring system – the motion may be strongly amplified and out of phase with the sea surface motion. For still shorter waves the motions will be opposed to the wave motion but less amplified, so when the crest of the wave passes the device the device will be at its lowest position, with obvious consequences for water overtopping the device or air penetrating under the bottom of the device. For very short waves the wave forces will be completely balanced by the inertia of the device itself and will show negligible motion.

In this report only the horizontal offset and motion will be treated for the purpose of using these in a quasi-static design approach.

1.2 Mooring Design Loop

The design loop a mooring system is outlined below.

a) Get metocean data for the site where the device will be positioned. Weather data may be taken from archived observations and satellite observations. Wave data can be "hindcasted" by wave generation models from historical meteorological data and also extrapolated by such models to places close to the coast from measurements at off-coast places. New measurements may then be started to check the results from the wave-generation models.

b) Settle design weather conditions.

c) Choose and apply methods for wind and current forces and some adequate wave force model.

d) Decide a preliminary mooring layout including number of mooring legs, dimensions of chains, ropes, buoys and clump weights.

e) Calculate static properties of the mooring system.

f) Calculate mean offset due to wind, current and mean wave drift forces.

g) Calculate the global, horizontal, linearized stiffness of the mooring system around the mean offset position.

h) Calculate the response motions

i) Derive the load effects i.e. the mooring-line tensions.

j) Repeat from point d) until the design rules are fulfilled.

1.3 On Wave-Induced Forces

One may say that there are two fundamentally different ways to calculate wave-induced forces on structures in the sea. In one method one considers the structure as a whole and assesses the total wave force from empirical or computed coefficients applied on water velocities and accelerations in

the undistorted wave motion. In the other method the pressure distribution around the surface of the structure is computed taking into account the effect on the water motion distorted by the structure itself, and subsequently integrated around the structure.

In both cases some mathematical model for describing the wave properties is necessary. For instance, by making the simplified assumption that the wave motion can be regarded as potential flow, velocities, accelerations and water motion can be computed in any point under a gravity surface wave by a scalar quantity, the velocity potential.

2 Design Rules and Guidelines

2.1 Quasi-Static Design

In modern quasi-static procedures, first, constant loads from mean wind, mean current and mean wave drift are assumed acting co-linearly on the moored floating object, as is stated in DNV-OS-E301 POSMOOR[v] of Det norske Veritas (DNV). This gives a mean horizontal offset in the load direction. The equation of motion – including the stiffness of the mooring system – is then solved so that possible resonance effects are taken into account. Sometimes, time-domain simulations with non-linear static mooring reaction are performed, but wave frequency and low-frequency motion responses may alternatively be calculated separately in the frequency domain and added. In the latter case, a horizontal, linearized mooring stiffness is used. In DNV-OS-E301 the larger of the below combined horizontal offsets is then used for calculation of quasi static line tension

$$X_{C1} = X_{mean} + X_{LF-max} + X_{WF-sig}$$
$$X_{C2} = X_{mean} + X_{LF-sig} + X_{WF-max} \qquad \text{Equation 2-1}$$

where X_{C1} and X_{C2} are the characteristic offsets to be considered, X_{mean} is the offset caused by the mean environmental loads and, $X_{LF\text{-}max}$ and $X_{LF\text{-}sig}$ are, respectively, the maximum and significant offset caused by the low-frequency loads and $X_{WF\text{-}max}$ and $X_{WF\text{-}sig}$ the maximum and significant offset caused by the wave-frequency loads. The low- and wave-frequency motions shall be calculated in the mean offset position using the linearized mooring stiffness in the mean position. By the index max is meant the most probable maximum amplitude motion in three hours. By the index sig is meant the significant amplitude motion in three hours. If the standard deviation of motion is σ, then the significant offset is 2σ , and the most probable maximum offset is $\sqrt{0.5\ \ln N}\,\sigma$ in N oscillations which means 1.86σ in 1000 waves (T_z = 11 s) and maybe 1.5 in in the slowly varying oscillations (N = 100, T_z = 110 s).

2.2 Allowed Tension in the Ultimate Limit State, ULS

The tension caused by the greater of the two extreme offsets according to Equation 2-1 is subsequently used to calculate the design tension in the most loaded mooring leg. For a conventional catenary system this would be in a windward mooring leg at the attachment point to the floating device.

In DNV-OS-E301 two consequence classes are introduced in the ULS and ALS, defined as:
Class 1, where mooring system failure is unlikely to lead to unacceptable consequences such as loss of life, collision with an adjacent platform, uncontrolled outflow of oil or gas, capsize or sinking.
Class 2, where mooring system failure may well lead to unacceptable consequences of these types.

The calculated tension $T_{QS}(X_C)$ should be multiplied by a partial safety factor γ = 1.7 for Consequence Class 1 and quasi-static design from Table 2-1 below, and the product should be less than 0.95 times the minimum breaking strength, S_{mbs}, when statistics of the breaking strength of the component are not available:

$$\gamma T_{QS} < 0.95 S_{mbs} \qquad \text{Equation 2-2}$$

or expressed by a utilization factor, u, which should be less than 1:

$$u = \frac{\gamma T_{QS}}{0.95 S_{mbs}} < 1 \qquad \text{Equation 2-3}$$

Table 2-1 Partial safety factors for ULS, DNV-OS-E301[v]

Consequence Class	Type of Analysis	Partial Safety Factor for Mean Tension	Partial Safety Factor for Dynamic Tension
1	Dynamic	1.10	1.50
2	Dynamic	1.40	2.10
1	Quasi-static	1.70	
2	Quasi-static	2.50	

2.3 Dynamic Design

In dynamic design, the time domain motion of the attachment points of the mooring cables is fed into some cable dynamics program to produce dynamic forces in the cables. This is especially vital for reproducing the maximum tensions in the cables. In Figure 2-1 as an example, time traces of measured cable tension, tension simulated in the cable dynamics program MODEX[vii] and tension calculated from the static elastic catenary are plotted, the latter two using the measured fairlead motion as input. A similar observation was made in analyses for the WaveBob[viii]. This was often referred to as Dynamic Design around 1990. In DNV-OS-E301[v] this is the standard procedure for the mooring line response analysis. Programs containing this approach are, e.g., MIMOSA[ix], ORCAFLEX[x], ZENMOOR[xi] and SIMO[xii]. SIMO, in combination with the cable dynamics program RIFLEX[xiii], has been used by Parmeggiano *an al.*[xiv] for the Wave Dragon.

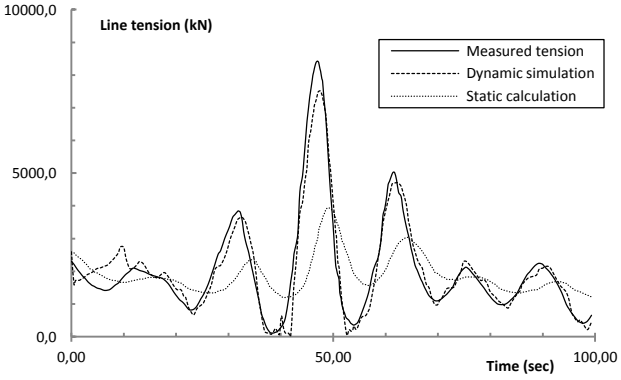

Figure 2-1
Course of cable tension around the time for maximum tension in a model test of GVA 5000P (Troll C) © 1987 Offshore Technology Conference[vii].

2.4 Coupled Analysis

In modern computer packages for mooring design "fully" coupled mooring analysis is often included, for example, DeepC[xiii], CASH[xv], Orcaflex[x]. In such analyses, the floater characteristics are first calculated in a diffraction program and then time-domain simulations are run using convolution techniques with "full" dynamic reaction from all mooring cables and risers. Time series of cable and riser tensions, floater motions, air gap, etc. are output. Typically, around 10 to 20 realisations for each combination of environmental conditions are run and statistics of platform motions and cable and riser forces are subsequently evaluated. Still, the wave-induced motion is based on small-amplitude wave theory and small-amplitude body motion and viscous effects may only be included

by drag formulations. This may be less inaccurate for large platforms, with moderate motions compared to their size, than for wave-energy devices. Fully coupled analysis is often used as a final check in the design, for example, for Thunder Horse[xvi], with a displacement of 130,000 tonnes. A fully coupled analysis of multiple wave energy converters in a park configuration is described Gao and Moan[xvii], and the PELAMIS team used Orcaflex for coupled analysis of the moorings[xviii].

2.5 Coupled Analyses with Potential or CFD Simulations

The next natural step would be to exchange the diffraction calculation of the floating body for a non-linear potential simulation with free surface[xix] or CFD RANS simulation also containing viscosity. Efforts in the latter direction for wave-energy devices are made by, for example, Palm *et al.*[xx] and by Yu and Li[xxi] 0. Processor times are still large, but are gradually becoming more affordable.

2.6 Response-Based Analysis

Recently, it has become common to check the final design that was based on some specified environmental load combination. This is done within the framework of a "response-based analysis" using long time series of real and synthesised environmental data. For instance, such an analysis was made for the Jack & St Malo semisubmersible for Chevron[xxii], with 145,000 tonnes displacement, even larger than the Thunder Horse. A representative, but synthesised, 424 year period of data for every hour (3.8 million time stamps) was used as a basis. From this basis, around 380 000 statistically independent "worst" events were selected. Running dynamic simulations on all these 380 000 events is impractical, so these events were first screened in quasi-static analyses and around 1900 events were selected with extreme responses above specified levels. Again, the selected 1900 events were simulated by dynamic runs in the program SIMO using a somewhat simplified input for current drag and viscous effects. Of the 1900 events, around 220 met higher extreme response levels. Finally, these 220 events were simulated in SIMO with an updated current drag model calibrated against model tests for each sea state. In a statistical analysis, the N-year response was calculated and compared to the responses of the N-year environmental design load combinations. In this case, the responses to the N-year design conditions were found to be worse or equal to the simulated N-year responses for both 100 and 1000 year return periods[xxiii]. It may be anticipated that this technique could be used for a last check of the design of ocean energy converters.

3 Metocean Conditions

3.1 Combinations of Environmental Conditions

The target probabilities of failure and return periods for extreme loads as given in DNV-OS-E301[v] (POSMOOR) are referred in Table 3-1 and Table 3-2. These will be used here as approved, although it may seem reasonable that the safety and reliability requirements for offshore hydrocarbon units exceed those that should be applied to floating ocean energy converters.

Table 3-1
Target Annual Probability of Failure, DNV-OS-E301.

Limit State	Consequence Class	Target Annual Probability of Failure
ULS	1	10^{-4}
	2	10^{-5}

Table 3-2
Return Periods for Environmental Loads, DNV-OS-E301.

Return Period		
Current	Wind	Waves
10	100	100

3.2 Waves

According to DNV-OS-E301[v], sea states with return periods of 100 years shall normally be used. The wave conditions shall include a set of combinations of significant wave height and peak period along the 100-year contour. The joint probability distribution of significant wave height and peak wave periods at the mooring system site is necessary to establish the contour line. If this joint distribution is not available, then the range of combinations may be based on a contour line for the North Atlantic. It is important to perform calculations for several sea states along the 100-year contour line to make sure that the mooring system is properly designed. Ship-shaped units are sensitive to low frequency motion, and consequently a sea state with a short peak period can be critical. How to choose sea states along the contour line is indicated in Figure 3-1. The same values for wind and current shall be applied together with all the sea states chosen along the 100-year contour. If it is not possible to develop a contour line due to limited environmental data for a location a sensitivity analysis with respect to the peak period for the 100 year sea state shall be carried out. The range of wave steepness criteria defined in DNV-RP-C205[xxiv] can be applied to indicate a suitable range of peak wave periods to be considered in the sensitivity analysis.

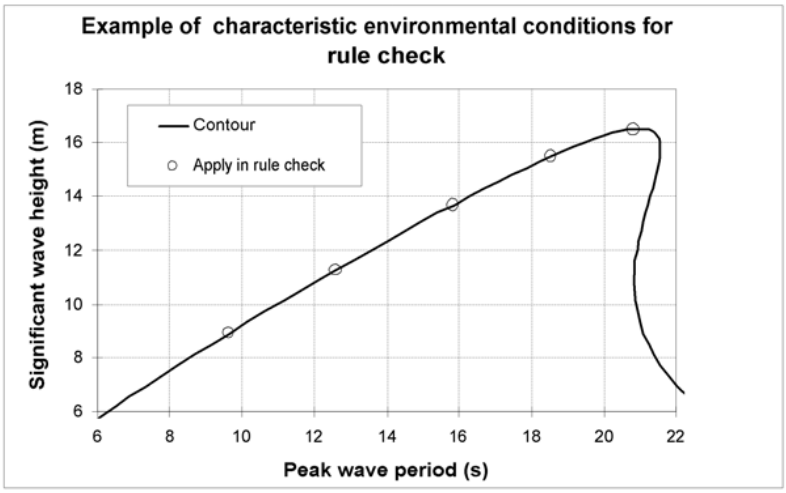

Figure 3-1
Selections of sea states along a 100-year contour line

In the guidance notes in POSMOOR some 100 year contour lines for offshore sites are given. However, they are not very useful in wave energy contexts as wave-energy sites are closer to the coast in shallower areas with milder wave climates. Therefore it is mostly necessary to use site-specific data, which can be created by using offshore data and a wave model as SWAN for transferring the deep water statistics to specific near-shore sites. Such data for Swedish waters are given e.g. by Waters et al.[xxv], Figure 3-2. This was simulated by help of WORLDWAVES[xxvi], which is a tool to assess the wave climate at a coastal or shallow water location, more or less anywhere in Europe, with acceptable accuracy and spatial resolution for most users. WORLDWAVES integrates several modules, including extensive offshore wave statistics, detailed bathymetry of the considered area, wave models to transfer the wave conditions to the desired near-shore location, and a statistical package for the evaluation of the near-shore wave statistics.

Measured data (E.g. Söderberg[xxvii]) for short periods has to be adjusted by comparing with long measurements at nearby sites and long, however, qualitative experience Sjöfartsverket[xxviii].

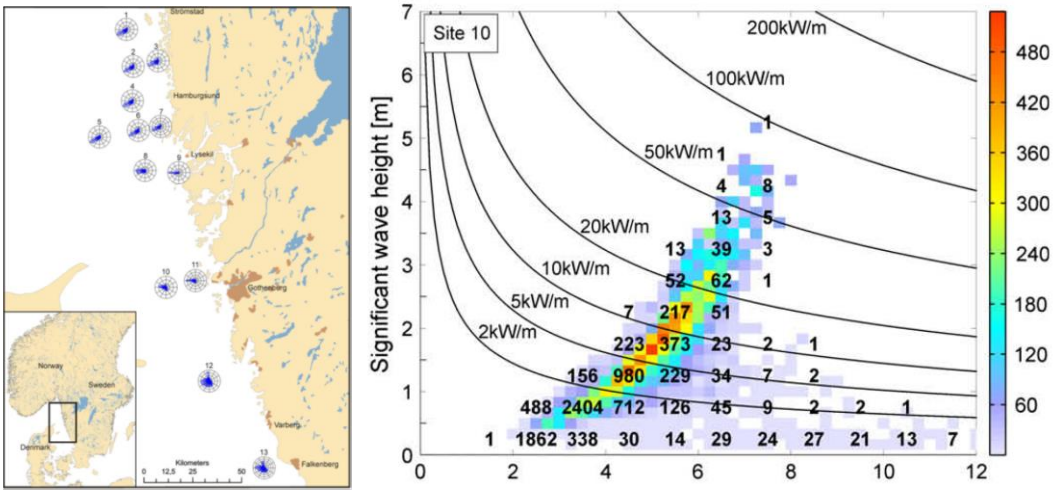

Figure 3-2
Combined scatter and energy diagrams for a site off Göteborg, No 10 in the chart to the left. Colours show annual energy transport per meter of wave front (kWh/(m year)). Numbers give average occurrence in hours per year. Isolines present the energy flux. (Waters *et al.*[xxv]) Energy period T_e on x-axis.

3.3 Environmental Data for Hanstholm

The example mooring design in this report is intended for a site off Hanstholm, Denmark. As a background available environmental data for Hanstholm are referred in the following.
Data are published by Margheritini on waves[xxix] and on water levels[xxx]. In the latter publication it is pointed out that statistics for wind and currents are missing. Margheritini concludes the wave data analysis by giving the extreme 100 year wave as H_s = 8.28 m for the 100 year return period. In accordance to standards, the range of the wave peak period T_p is given by:

$$\sqrt{\frac{130H_s}{g}} < T_p < \sqrt{\frac{280H_s}{g}} \qquad \text{Equation 3-1}$$

The extreme wave conditions for other return periods have been calculated and are referred in Table 3-3. The water depth at the measuring site is given as 17.5 m, which would give depth limited 100 year waves at this site, $H < 0.78h_d$ = 13.7 m, but at the intended site for the example wave-energy buoy the water depth is 30m, why the waves at this site is not depth limited .

Table 3-3 Extreme waves at Hanstholm[xxix]

Return Periods [y]	Significant wave height [m]
1	5.56
2	6.05
5	6.63
10	7.04
20	7.43
50	7.92
100	8.28

Sterndorf[xxxi] has made some conclusions about the environmental data from similar data sources. The design wave data is predicted for a water depth of 11 m closer to land than the wave measurements that in this case were performed at the 30 m contour but in shelter of a shallower area with a water depth of 20 m. See Table 3-4. In Figure 3-3 the design 3-hour $H_s - T_z$ contour at 11 m water depth at Hanstholm is given as proposed by Sterndorf.

Table 3-4 Design wave conditions (11 m water depth) (Sterndorf[xxxi])

Probability of exceedence	Significant Wave Height in Deep Water for Waves coming from				
	SW	W	NW	N	NE
$H_{s,3\ hours}$ - 1 Year [m]	4.1	4.7	4.8	4.1	3.0
$H_{s,3\ hours}$ - 10 Year [m]	5.0	5.6	5.8	5.2	3.9
$H_{s,3\ hours}$ – 100 Year [m]	5.8	6.5	6.6	6.1	4.5

Table 3-5 Design wind conditions (Sterndorf[xxxi])

Probability of exceedence	Wind Speed for Wind coming from				
	SW	W	NW	N	NE
$V_{wind,3\ hours}$ - 1 Year [m/s]	21.0	25.0	25.0	19.0	20.0
$V_{wind,3\ hours}$ - 10 Year [m/s]	24.0	30.0	29.5	23.5	25.0
$V_{wind,3\ hours}$ – 100 Year [m/s]	28.0	34.0	33.0	28.0	29.0
Probability of wind direction	15.5%	18.4%	11.8%	5.2%	8.4%

Table 3-6 Design water levels (Sterndorf[xxxi])

Probability of exceedence	High Water	Low Water
3 hours 1 year	1.22 m	1.28 m
3 hours 10 year	1.58 m	1.52 m
3 hours 100 year	1.96 m	1.78 m

Sterndorf[xxxi] estimates the current to 3 % of the wind speed, assuming the current to be locally wind generated, yielding 0.68 m/s from SW and 0.58 m/s from NE, while Margheritini[xxx] cites measured values at 0.5-1.5 m/s coast parallel. Sterndorf gives the wind speed as $V_{wind,\ 3\ hours}$, but normally the 10 min mean value is used for mooring design of floating objects.

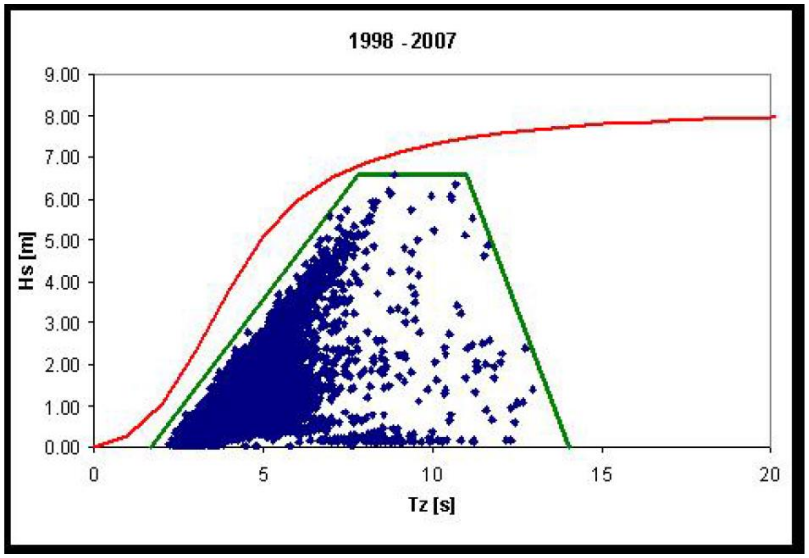

Figure 3-3

Design 3-hour H_s – T_z contour at 11 m water depth at Hanstholm
suggested by Sterndorf[xxxi]. Compare to Figure 3-1

3.4 Chosen Design Conditions

In the sample design calculations below the following values are chosen:

Mean wind speed is taken from Table 3-5:
100 year return period: $U_{10\text{min},10\text{m}}$ = 33 m/s
However it may be argued that it should be higher as this is given as the three-hour mean wind by Sterndorf.

Mean current velocity is set to the maximum measured value according to Margheritini. See text below Table 3-6:
10 year return period: U_c = 1.5 m/s

Waves are taken from Table 3-3:
100 year return period: H_s = 8.3 m,
a standard PM-spectrum gives then T_p = 12.9 s and T_z = 10.1 s
The 3 h most probable maximum wave is then around $H_{max} = H_s\sqrt{0.5\ln(3\text{h}/T_z)}$ = 15.4 m

Wind, current and waves in the same direction

Water depth is taken as h_d = 30 m from Pecher *et al.* [xxxii]

3.5 Sample Floater

In this report we will illustrate the methods by applying them to a floating, moored, vertical, truncated, circular cylinder.

Table 1-1 Properties of the sample floater

Diameter (m)	5
Height above mean water surface	5
Draught (m)	5
Mass (tonne)	100
Pitch inertia around mean water surface (tonne m²)	1 830
Cross coupled inertia ($m_{24} = m_{42} = -m_{15} = -m_{51}$ (tonne m)	243

4 Estimation of Environmental Loads

It is demanding to establish the hydrodynamic loads for wave-energy-devices, because they may undergo very large resonant motion, have very complex shapes composed of articulated connected bodies or involve a net flow of water through the device. This makes it difficult to use conventional potential methods. Probably, most devices need undergo extensive tank and field testing. However, here we will sketch simplified methods for first estimates of loads useful in the concept stage and for planning tank tests.

4.1 Mean Wind Load and Sea Current Load

According to DNV-OS-E301[v] the wind and current load should be determined by using wind tunnel tests. Wind loads from model basin tests are only applicable for calibration of an analysis model, while the current loads may be estimated from model basin tests or calculations according to recognised theories (DNV-RP-C205[xxiv], Section 6). In preliminary design also wind loads calculated according to recognised standards may be accepted, such as in DNV-RP-C205[xxiv], Section 5.

The mean wind and drag force may be calculated using a drag force formulation, with drag coefficients from model tests, or numerical flow analysis. Mean wind forces described with a wind profile, and oscillatory wind forces due to wind gusts shall both be included. Wind profile according to DNV-RP-C205[xxiv] and ISO19901-1 shall be applied.

$$F = CA\frac{1}{2}\rho U^2 \qquad \text{Equation 4-1}$$

Here C is traditionally called the shape coefficient for wind force calculations and drag coefficient for current force calculations, A is the cross sectional area projected transverse the flow direction, ρ is the density of the fluid and U is a time mean of the fluid velocity at the height of the centre of the exposed body. Here we will use the design 10 minute mean for the air velocity and the design value of the current, as the response of the horizontal motions and the induced mooring tension are in this time scale.

Values on the coefficient C for different shapes are given in DNV-RP-C205[xxiv], but can also be found in other standard literature like Faltinsen[xxxiii], Sachs[xxxiv]. For more complicated superstructures a discussion is found in Haddara and Guedes-Soares[xxxv]. In DNV-RP-C205 there are also guidelines for calculating vibrations or slowly varying wind load due to a wind spectrum. This is out of scope of this report.

4.1.1 Wind and current loads on the floaters

Below the calculation of the wind and current forces are sketched but more detailed information can be found in DNV-RP-C205.

4.1.1.1 Wind load on the buoy:

Mean wind speed $U_{10\,min\,,10\,m}$ = 33 m/s
To use the drag-force expression Equation 4-1 for the wind load we must first estimate the wind speed at the centre of the buoy which is situated 2.5 m above the mean-water surface. The wind is given at 10 m height. A wind gradient expression giving the wind speed at 2.5 m from the value at

10 m gives

$$U(2.5\text{ m}) = U(10\text{ m})\left(\frac{2.5\text{ m}}{10\text{ m}}\right)^{0.12} = U(10\text{ m})0.85 = 28.9\frac{\text{m}}{\text{s}} \qquad \text{Equation 4-2}$$

In order to estimate the shape coefficient *C* from graphs and tables in DNV-RP-C205 we must also calculate the Reynolds number

Reynolds No $Re = \frac{U_{T,z}D}{\nu_a} = 9.6 \cdot 10^6$

where D = 5 m is the diameter, ν_a is the kinematic viscosity ν_a = 1.45x10^{-5} m^2/s (DNV-RP-C205[xxiv], APPENDIX F)

Figure 6-6 in DNV gives C = 1.1 for a relative roughness of 0.01.

The aspect ratio is $2h_b/D$ = 2 and gives a reduction factor of κ = 0.8 for supercritical flow. The height above the water surface of the buoy, h_b, is the same as the diameter, D, and it is considered as mirrored in the water surface to calculate the aspect ratio, which is defined as the length over width ratio.

Air density ρ_a = 1.226 kg/m^3 at 15ºC.

Thus the wind force is

$$F_a = \kappa C D h_b \frac{1}{2}\rho U_{T,z}^2 = 10.5\text{ kN} \qquad \text{Equation 4-3}$$

4.1.1.2 Current load on the buoy:

The current speed is assumed to have no vertical gradient close to the free water surface:
mean current speed U_c = 1.5 m/s

In order to estimate the drag coefficient C from graphs and tables in DNV-RP-C205 we must estimate the Reynolds number:

Reynolds No $Re = \frac{U_c D}{\nu_w} = 6.3 \cdot 10^6$

where D = 5 m is the diameter, ν_w is the kinematic viscosity ν_w = 1.19x10^{-6} m^2/s

Figure 6-6 in DNV gives again C = 1.1 for a relative roughness of 0.01

The aspect ratio is $2D_b/D$ = 2 and gives a reduction factor of κ = 0.8 for supercritical flow. The draught below the water surface of the buoy, D_b, is the same as the diameter, D, and again it is considered as mirrored in the water surface to calculate the aspect ratio.

Sea water density ρ_w = 1025.9 kg/m^3 at 15ºC

Thus the current force is

$$F_c = \kappa C D D_b \frac{1}{2}\rho U^2 = 24.5\text{ kN} \qquad \text{Equation 4-4}$$

4.2 Wave Loads

4.2.1 Mean wave drift force in regular waves, simplified approach

Basically there are two alternative approaches to estimate the wave-drift force. The first approach involves integrating the pressure over the instantaneously wetted surface of the body. This will, for a body in a regular wave, give a force composed by a mean force, a force at the same frequency as the incident wave (the usual first-order wave force, which will be discussed in the next paragraph) and a force at the double frequency. For the slowly varying drift forces only the mean force is of interest. The second approach involves utilising the momentum conservation and will be used here[xxxvi]. We will sketch it for a 2D body in a plane, unidirectional wave motion with the incident wave amplitude *a*.

Through a vertical the time mean of the incident momentum is

$$I_0 = \frac{\rho g a^2}{4} \qquad \text{Equation 4-5}$$

If this wave is blocked by a vertical wall, a wave with the same amplitude, $r = a$, will be reflected in the opposite direction and the momentum acting on the wall, or mean drift force will become

$$F_d = I_{in} - I_{out} = \frac{\rho g}{4}(a^2 + r^2) = \frac{\rho g a^2}{2} \qquad \text{Equation 4-6}$$

This is the largest possible mean wave drift force on a floating body per unit width of structure. For a floating 2D body, however, only a fraction of the energy will be transmitted and the body will be set in motion and radiate energy up-wave and down-wave. If we denote the amplitude of the combined reflected and back-radiated wave by *r* and the amplitude of the combined transmitted and down-wave radiated wave by *t*, then a momentum approach will give

$$F_d = \frac{\rho g}{4}(a^2 + r^2 - t^2) \qquad \text{Equation 4-7}$$

This was set up by Longuet-Higgins[xxxvi]. Maruo[xxxvii] stated that if there are no losses in the flow, the sum of the powers in the *r* wave and the *t* wave must equal the power in the incident wave, i.e. $(a^2 = r^2 + t^2)$ and consequently

$$F_d = \frac{\rho g}{2} r^2 \qquad \text{Equation 4-8}$$

For successful wave-energy devices this equation is not valid, as then $a^2 \gg r^2 + t^2$.

For real devices with limited transverse extension the above equations can be seen as upper bounds as the wave is scattered around the object and waves are radiated by the object in the horizontal plane.

4.2.2 Mean wave drift load in irregular waves

A very simple approach on the conservative side is based on the assumption that the object reflects all waves in the opposite direction to the incoming waves for all component waves, with the amplitude, a_i. In e.g. a PM-spectrum with H_s = 8.3 m the drift force would be:

$$F_d = \frac{1}{2}\rho g \sum_i \frac{1}{2} a_i^2 D = \frac{\rho g {H_s}^2}{32} D = 108 \text{ kN} \qquad \text{Equation 4-9}$$

This is four times the current force. However, normally, a floating buoy would not reflect components in the spectrum with wave-lengths larger than around 5 diameters, in our case $5 \cdot D = 20$ m, which corresponds to a wave period longer than around $T = 3.6$ s or a frequency less than 0.28 Hz. This is because the buoy would just follow the moving wavy surface without causing any disturbance, except at resonance frequencies. For shorter waves say wave-lengths less than D/5 corresponding to < 4 m, < 1.6 s or > 0.6 Hz on the other hand the waves would be totally reflected by a 2D body or scattered by a buoy because the buoy will not oscillate with the waves. Equation 4-9 above presumes that all components would be reflected without any scatter. Plotting a PM-spectrum with $H_s = 8.3$ m and drawing the line for $T = 3.6$ s gives the following picture that indicates that the wave drift force would be negligible, as almost the entire spectrum is below this frequency.

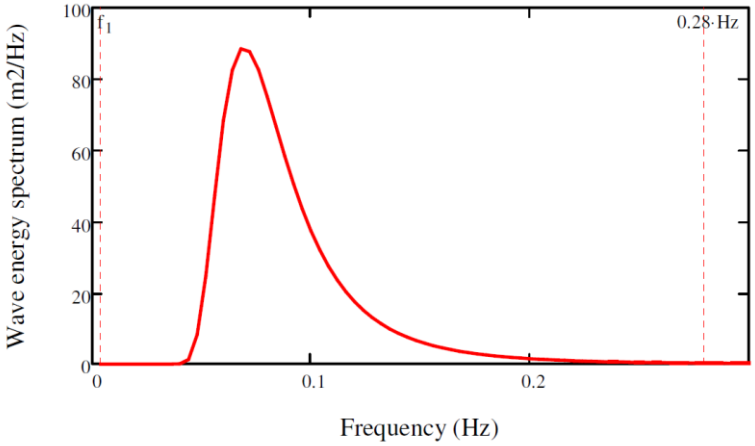

Figure 4-1
The design wave energy spectrum, PM-spectrum with $H_s = 8.3$ m.
The wave period 0.28 Hz corresponding to a wave length of 5 *D* is marked in the figure.

To check that the drift force really is small in the survival design storm with $H_s = 8.3$ m, we have calculated the drift force coefficient with WADAM[xiii] and integrated the total drift force in that sea state. See Figure below. Using WADAM's definition of the drift-force coefficient, the drift force can be written

$$F_d = 2\rho g D \sum_i C_{d_i} \frac{1}{2} a_i^2 \qquad \text{Equation 4-10}$$

The resultant drift force was found to be $F_d = 2.5$ kN, which in this case is 25 % of the estimated wind force and 10 % of the current force and can thus − as a first approximation − be neglected in the design storm. In operational sea states with shorter waves and lower wave heights the drift force may be of the same magnitude as the wind and current forces, but all the forces are smaller.

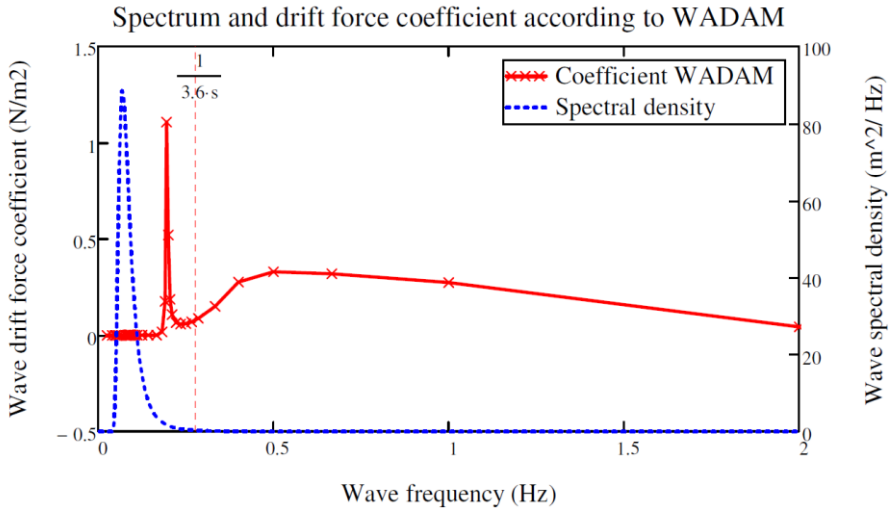

Figure 4-2
The drift force coefficient as a function of wave frequency as calculated by WADAM[viii].
Note the effect of the vertical resonant motion at 0.2 Hz.

4.2.3 First-order wave forces

4.2.3.1 Wave forces on ”small” bodies *D<L/5*

The first approach to calculating wave forces on bodies in water was founded on the assumption that the body does not affect the water motion and pressure distribution in the incident wave. Nowadays one would normally use diffraction theory, taking into account the scatter of the incident wave caused by the body.

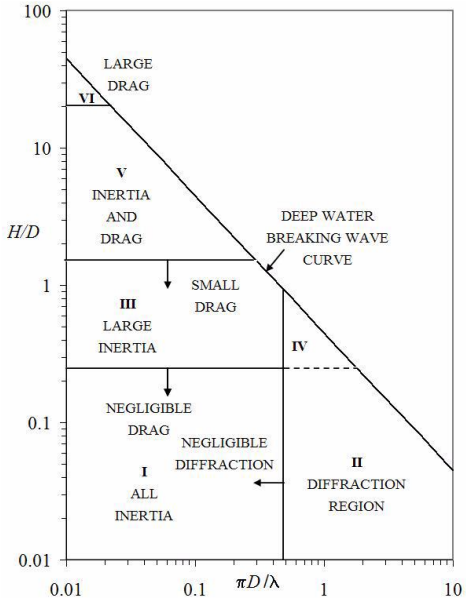

Figure 4-3
Different wave force regimes (Chakrabarti, 1987, cited by DNV).
D = characteristic dimension, H = sinusoidal wave height, λ = wave length.
From DNV-RP-C205[xxiv].

In Figure 4-3 above we can note different flow regimes as function of $\pi D/\lambda$ and H/D. In the buoy case $\pi D/\lambda = \pi D/(g\ T_p^2/2\pi) \approx 0.06$ and $H_{max}/D \approx 3$, which set us in the inertia and drag regime. For such bodies with a characteristic diameter of less than 1/4 to 1/5 of a wave length the effect on the

wave is small, and the wave force can, as an approximation, be set to the sum of an inertia term and a drag term. The inertia term is the product of the displaced mass, added mass included, and the undisturbed relative water acceleration in the centre of displacement. The drag term depends on the relative velocity between water and body. In surge this so called Morison formulation is:

$$F = \rho V \frac{du}{dt} - m\ddot{x} + C_m \rho V \left(\frac{du}{dt} - \ddot{x}\right) + \frac{1}{2} C_D \rho A |u - \dot{x}|(u - \dot{x}) \qquad \text{Equation 4-11}$$

where F is the reaction force from e.g. a mooring system (Unmoored body $F = 0$),
ρ is the density of water,
V the displaced volume,
u and $\frac{du}{dt}$ the undisturbed horizontal water velocity and acceleration in the centre of the body,
m the mass of the body,
x the horizontal position of the body,
$\ddot{x}$ and $\dot{x}$ the acceleration and velocity of the body,
C_m an added mass coefficient (Can be taken from standard values in e.g. DNV-RP-C205[xxiv]),
C_D a drag coefficient (Can be chosen from recommendations in e.g. DNV-RP-C205) and
A the cross-sectional area in the direction perpendicular to the relative velocity

So far we have not defined any properties of the mooring system, but for the time being we can assume that the body is fixed to select the coefficients C_m and C_D, again using DNV-RP-C205[xxiv]. One should then take into account the variation of C_D and C_m as functions of the Reynolds number, the Keulegan-Carpenter number and the relative roughness.

Reynolds number: $Re = u_{max}\, D/\nu$
Keulegan-Carpenter number: $KC = u_{max}\, T/D$
Relative roughness: k/D

where D = diameter = 5 m
T = wave period = T_p = 12.9 s
k = roughness height = 0.005 m
u_{max} = maximum water velocity in a period $\pi H_{max}/T_p$ = 3.8 m/s (assuming circular water motion in deep water) and
ν_w = 1.19x10^{-6} m^2/s = fluid kinematic viscosity.

For the buoy $Re = 8 \cdot 10^6$, KC = 10 and k/D = 10^{-3}. For coefficients of slender structures DNV-RP-C205 still refers to Sarpkaya and Isacson[xxxviii] (1981) but the problem is that their graphs and experience are limited to Re < $15 \cdot 10^5$. See also Chakrabarti[xxxix] (2005). Anyway, these graphs and also equations in DNV-RP-C205, Paragraph 6.7, point to $C_D = 1$ and $C_m = 1$ for circular cylinders. As before the drag coefficient may be reduced to 0.8 due to the aspect ratio. In Appendix D, RP-C205, Table D-2 there is also an indication that C_m could be reduced to around 0.8 due to the aspect ratio $L/D = 2$

Applying the Morison equation above for the fixed body, it reduces to

$$F = \rho V (1 + C_m) \frac{du}{dt} + \frac{1}{2} C_D \rho A |u| u. \qquad \text{Equation 4-12}$$

This force as a function of time for the wave amplitude $a = H_{max}/2$ is drawn in the figure below together with the horizontal water acceleration, and one can note that the evolution in time is

affected by the drag, but that the maximum value is almost unaffected, and can approximately be calculated as

$$F_M = \rho V(1 + C_m)\frac{du_a}{dt}_{max} = 0.44 \text{ MN}, \qquad \text{Equation 4-13}$$

in spite of the fact that we are in the inertia and drag regime. $F_M = \pm 0.44$ MN are also drawn as horizontal lines in the graph. The drag-force maximum is F_D = 0.3 MN but is 90 degrees out of phase with the acceleration and in phase with the velocity.

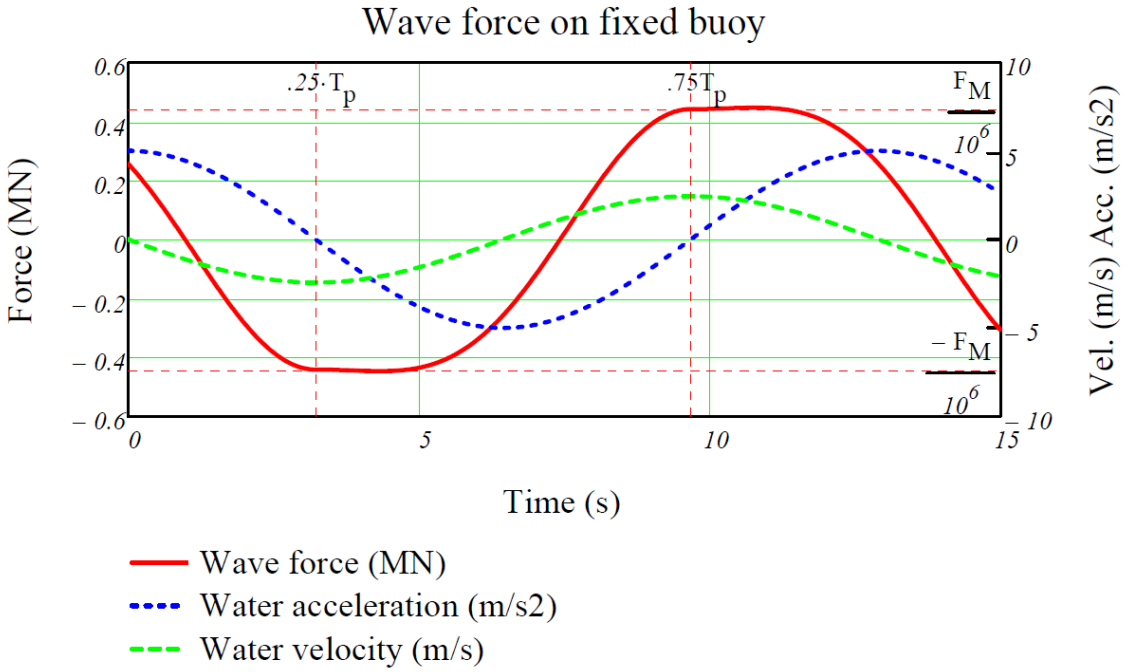

Figure 4-4
The Morison force as a function of time for the wave amplitude a = H_{max}/2 and period T_p = 12.9 s. The water acceleration is drawn for comparison.

We can note that the wave force amplitude is one order of magnitude larger than the mean load from wind, current and wave drift. However, for a floating moored body the wave load should be carried by the inertia of the body and not by the mooring or positioning system as we do not want to counteract the wave-induced motion only prevent the buoy from drifting off its position.

Wave forces in irregular waves (Small body)

If we drop the drag term in the wave force equation above, we may think we can calculate the wave force spectrum, $S_F(f)$, directly by multiplication of the wave spectrum, $S_{PM}(f)$ by the square of the wave force ratio, $f_w(f)$. The problem is that for f > 0.28 Hz the diffraction would be important and the small body assumption is not valid. The force amplitude divided by the wave amplitude or force amplitude ratio would become

$$f_w(f) = \frac{F}{a} = \frac{\rho V}{a}(1 + C_m)\frac{du}{dt}_{max} = \rho V(1 + C_m)gk\frac{\cosh(k(z+h))}{\cosh(kh)} \quad f < 0.28 \text{ and}$$
$$f_w(f) = 0 \quad f > 0.28. \qquad \text{Equation 4-14}$$

The wave force spectrum could then be calculated as

$$S_F(f) = \left(f_w(f)\right)^2 S_{PM}(f) \qquad \text{Equation 4-15}$$

These functions are drawn in Figure 4-1

The significant force amplitude is then

$$F_{Msamp} = 2\sqrt{m_{0F}} = 2\sqrt{\int_{0\ \mathrm{Hz}}^{0.28\mathrm{Hz}} S_F(f)df} = 0.38\mathrm{MN} \qquad \text{Equation 4-16}$$

And the maximum force in 3 h would be $F_{Mmax} = 1.86\ F_{Msamp}$ = 0.71 MN.

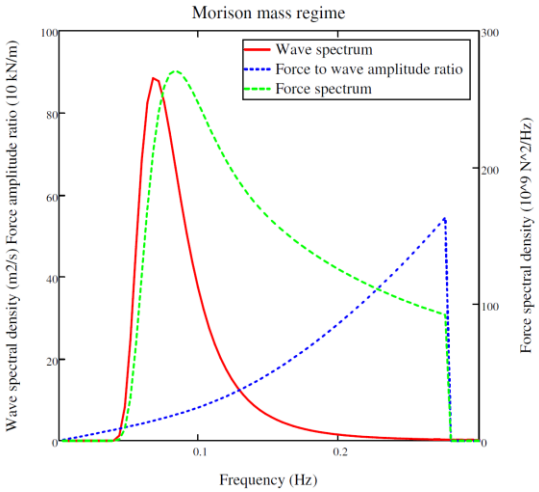

Figure 4-5
Wave energy spectrum, $S_{PM}(f)$, force amplitude ratio, $f_w(f)$, and force spectrum, $S_F(f)$. Morison approach.

4.2.3.2 Wave forces on ”large” bodies

To extend the force calculation to shorter waves or relatively larger bodies (Figure 4-2) we are forced to use diffraction theory, which is more demanding and, yet, does not take drag (viscous) forces into account. On the other hand radiation damping caused by waves generated at the motion of the body in or close to the free surface are included, which lacks in the Morison approach. For the diffraction problem of the vertical circular buoy there are analytical series solutions available e.g. in Yeung[xl] and Johansson[xli]. Here, we will illustrate the difference to the Morison approach by applying results from Johansson. Bodies with general form can be calculated in panel diffraction programs like WAMIT[xiii].

In the figures below graphs with added mass, radiation damping and wave force amplitude ratio as functions of frequency are displayed. The wave force amplitude ratio will be used immediately for comparison of wave forces on the fixed body. The added mass and radiation damping will be used later for calculating wave motion and slowly varying wave drift motion of the moored buoy.

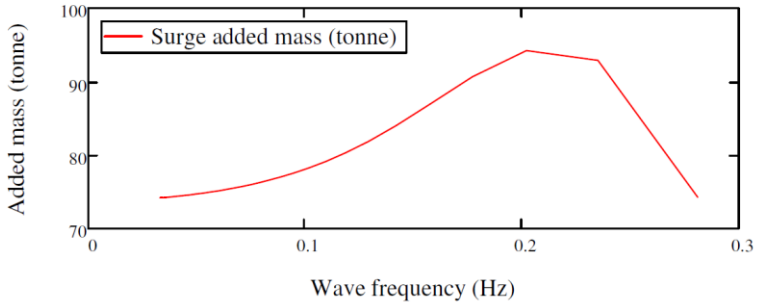

Figure 4-6
Surge added mass, A_{11}, as a function of wave frequency

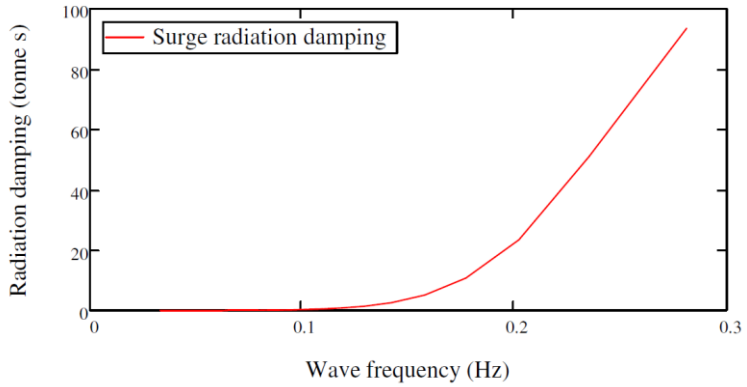

Figure 4-7
Surge radiation damping, B_{11}, as a function of wave frequency.

Wave forces in irregular waves (Large body)

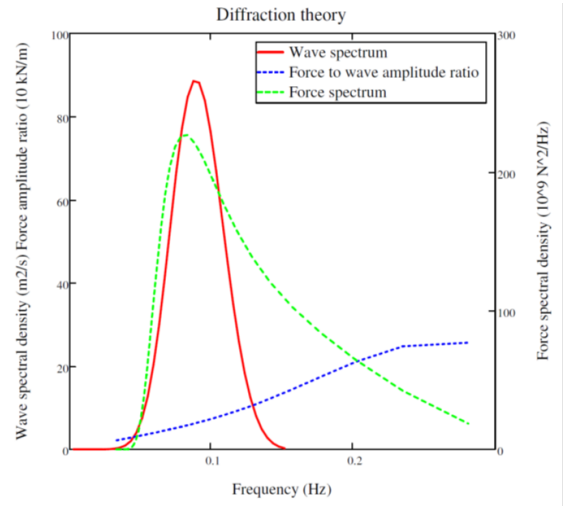

Figure 4-8
Wave energy spectrum, $S_{PM}(f)$, force amplitude ratio, $f_{dw}(f)$, and force spectrum, $S_{dF}(f)$. Diffraction results from Johansson[xli].

The wave force spectrum can now be calculated as before but with diffraction results instead of approximate coefficients

$$S_{dF}(f) = \left(f_{dw}(f)\right)^2 S_{PM}(f) \qquad \text{Equation 4-17}$$

The significant force amplitude is now estimated as

$$F_{dsamp} = 2\sqrt{m_{0dF}} = 2\sqrt{\sum_i S_{dF}(f_i)\Delta f_i} = 0.30\text{MN} \qquad \text{Equation 4-18}$$

And the maximum force in 3 h would be $F_{dmax} = 1.86\, F_{dsamp}$ = 0.55 MN.

The 23 % reduction of the force is due to the lower force amplitude ratio according to the diffraction theory compared to the Morison model. Note especially that the diffraction force ratio has a maximum around 0.3 Hz in this case and actually will decrease for higher frequencies while the Morison counterpart grows to infinity.

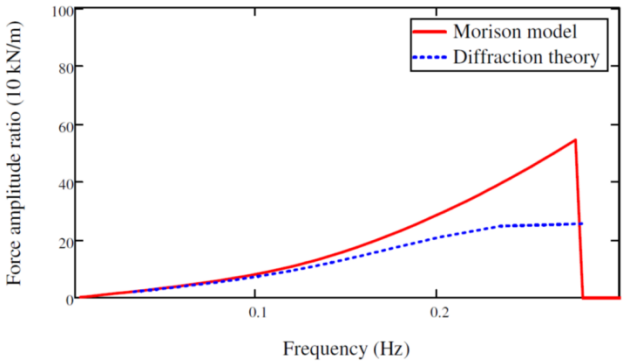

Figure 4-9
Force amplitude ratio according to the Morison approach and diffraction theory.

In the quasi-static mooring design approach we need estimate the motion of the moored object in regular design waves or in an irregular sea state. To get the mooring force we must know the statics of the mooring system, which will be outlined in the next chapter.

4.3 Summary of Environmental Loads on Buoy

In Table 4-1 there is a summary of results from the gradually more sophisticated calculations. First one can note that – in this case – the simplest wave-drift estimate gives 40 times as large value as the one founded on diffraction theory. This is important in relation to the wind and current force. The Morison wave force for a regular sinusoidal wave is very dependent on the assumed wave period, while the Morison approach for irregular waves gives some better significance, however some 20 % overestimation.

Table 4-1
Key results from load estimates on the floating buoy

Mean loads		Force (kN)
Wind	33 m/s	10.5
Current	1.5 m/s	24.5
Wavedrift H_s = 8.2 m	Simple	108
	Diffraction	2.5
Total mean	Simple	143
	Diffraction	37.8

Wave force	Force (MN)	
Morison Regul. $H_{max}/2$ = 7.7 m	0.44	Amplitude
Morison mass regime Irreg. H_s = 8.2 m	0.38	Significant
	0.71	Most prob. maximum
Diffraction Irreg. H_s = 8.2 m	0.30	Significant
	0.55	Most prob. maximum

5 Mooring system static properties (force displacement relations)

For illustrative purposes a mooring configurations will be used as presented by Pecher et al. (2014)[xxxii]: a three-leg Catenary Anchor Leg Mooring system, CALM. See Figure 5-1.

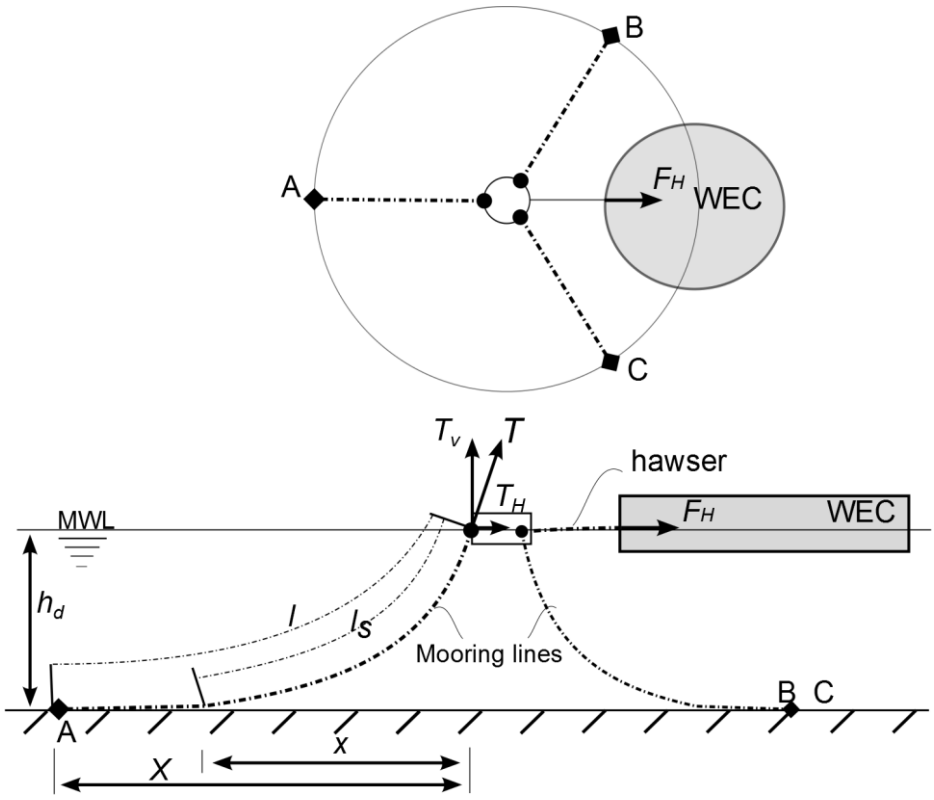

Figure 5-1
Sketch of a three-leg Catenary Anchor Leg Mooring, CALM, system[xxxii].

The CALM system is composed of three chain mooring legs directly fastened to the example buoy. This is different to the example by Pecher *et al.*[xxxii] who have assumed that the mooring legs are connected to a mooring buoy, which in turn is coupled by a hawser to a wave-energy device. The legs have equal properties listed in Table 5-1. The lengths of the mooring lines are chosen such that they will just lift all the way to the anchor when loaded to their breaking load.

Table 5-1
The CALM system

Three-leg system 120 deg	Chain Steel grade Q3	Notation
Water depth	30 m	h_d
Horizontal pretension	20 kN	T_o
Unstretched length	509 m	s
Breaking load	2014 kN	T_B
Diameter	50.4 mm	
Mass per unit unstretched length	53.65 kg/m	q_o
Weight in sea water per unit unstretched length	457 N/m	γ_r
Axial stiffness	228 MN	$K = EA$

5.1 Catenary Equations

Here we will use the equations for an elastic catenary expressed in the unstretched cable coordinate from its lowest point, or from the touch-down point at the sea bottom as in Figure 5-1, to a material point, s_o. (Ramsey[xlii], 1960).

The horizontal stretched span or the horizontal distance, $x_{o1}(s_o)$, from the touch-down point, $s_o = 0$, is

$$x_{o1}(s_o) = a \operatorname{arcsinh}\left(\frac{s_o}{a}\right) + \frac{\gamma_r a}{K} s_o, \qquad \text{Equation 5-1}$$

and the vertical span is

$$x_{o2}(s_o) = \sqrt{a^2 + s_o^2} + \frac{\gamma_r}{2K} s_o^2 - a, \qquad \text{Equation 5-2}$$

where $a = H/\gamma_r$ *i.e.* the horizontal force divided by the unstretched weight per unit length in water. Solving for the lifted cable length, s_o, for $x_{o2}(s_o) = h_d$ = the water depth, we can now express the total distance to the anchor including the part of chain resting on the sea floor as a function of the horizontal force, *H*.

$$X(H) = x_{o1}(s_o(H)) + (s - s_o(H))(1 + \frac{H}{K}), \qquad \text{Equation 5-3}$$

or inversely the horizontal force as a function of the stretched span $H(X)$, Figure 5-3

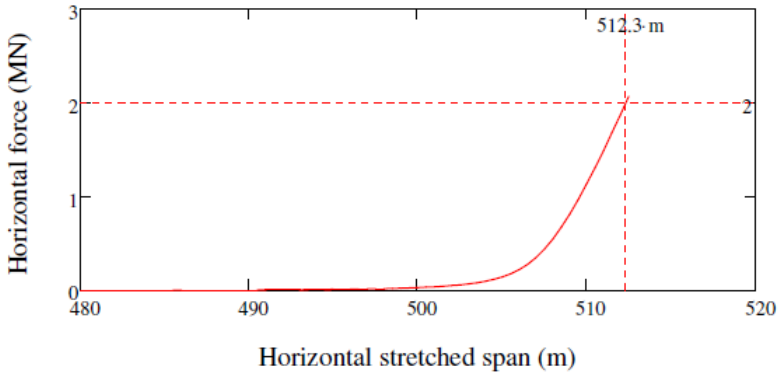

Figure 5-2
The horizontal force as a function of the horizontal stretched span.

In the intended system we have assumed a pretension of H_p = 20 kN at zero excursion. This corresponds to a horizontal span of $X(H_p)$ = 498.36 m. Finally we can add the reaction of the three legs to get the total horizontal mooring force as a function of the excursion, $x = X(H) - X(H_p)$, in the x-direction in parallel to the upwind leg.

$$F_{tot}(H) = H(x) - 2\cos(60°)H(-\frac{x}{\cos(60°)}), \qquad \text{Equation 5-4}$$

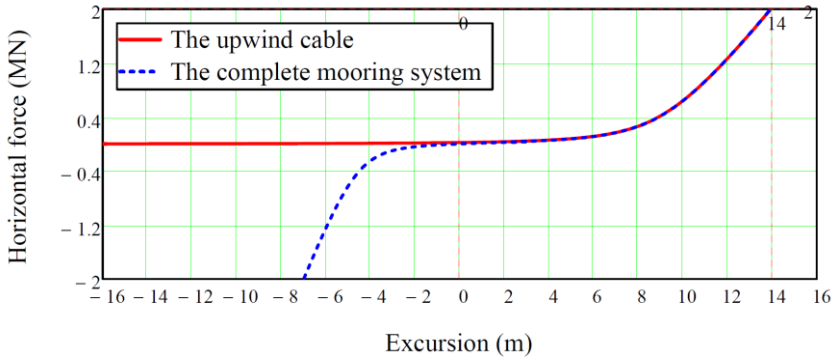

Figure 5-3
Horizontal force as a function of the excursion of the buoy.
The up-wave cable takes most of the load.

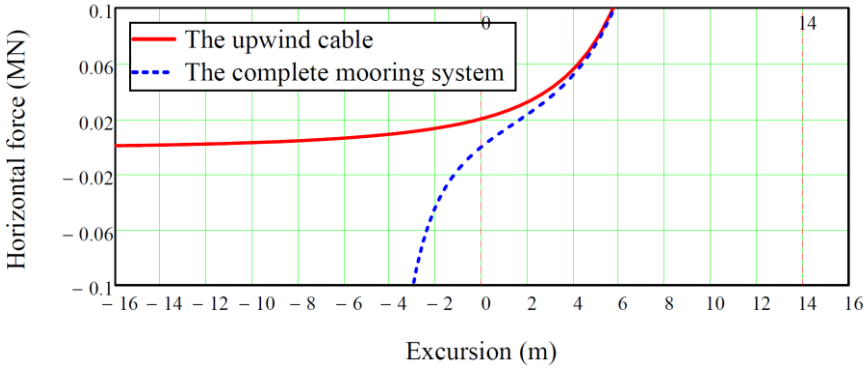

Figure 5-4
Horizontal force as a function of the excursion of the buoy.
Different range of vertical axis compared to Figure 5-3

In the example we can see that almost all the horizontal load is carried by the cable in the up-wave direction as soon as the excursion exceeds 4 m.

Last we need calculate the horizontal stiffness, $S(x)$, of the mooring system, that is, the slope of the function displayed in Figure 5-4 and Figure 5-5.

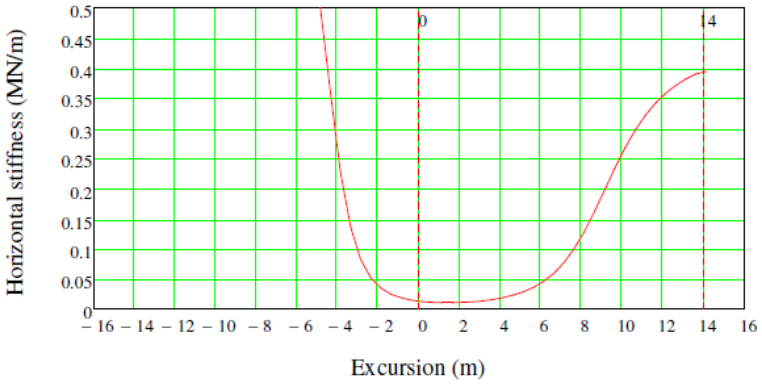

Figure 5-6
The horizontal stiffness of the mooring system as a function of the excursion.

It is interesting to note that the stiffness for negative excursion is larger than for positive excursion, which is caused by having two interacting legs in this direction.

5.2 Mean Excursion

The horizontal motion should be calculated around the mean offset (excursion). Therefore the offset due to the mean forces is calculated using the methods described above. We also need the mooring stiffness around the mean offset. The results are given in Table 5-2.

Table 5-2
Summary of offset and mooring stiffness due to the mean environmental forces

Mean force	Force (kN)	Mean offset (m)	Tangential Stiffness (kN/m)
Wind+current+Maximum wave drift	10.5+24.5+108 = = 143	6.45	68
Wind+current+WADAM wave drift	10.5+24.5+2.5 = = 37.5	2.63	12

6 Response Motion of the Moored Structure

6.1 Equation of Motion

The loads on a floating body can be constant as the mean load in Paragraph 5.2, transient i.e. of short duration or harmonic. Irregular or random loads from e.g. sea waves can to a first, linear approximation be treated as a superposition of harmonic loads, an approach that will be used here. The responses are fundamentally different for the three types of loads. The present buoy – mooring system will be treated as a single-degree-of-freedom (SDoF) system as illustrated in Figure 6-1.

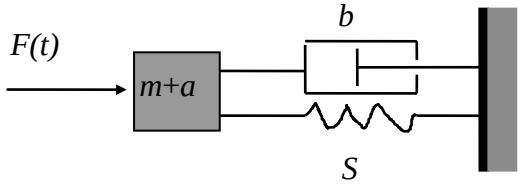

Figure 6-1
A mechanical system with one degree of freedom, mass, *m*, added mass, *a*, damping coefficient, *b*, and spring stiffness, *S*.

The equation of motion for this system can be written

$$(m+a)\ddot{x} + b\dot{x} + Sx = F(t) \qquad \text{Equation 6-1}$$

For bodies in water the mass inertia is increased by an ”added mass”, *a*, or hydrodynamic mass. In our case this is represented by the C_m coefficient. This is a result of the fact that to accelerate the body it is also necessary to accelerate the water surrounding the body. For submerged bodies close to the water surface the added mass can be negative, but for deeply submerged bodies it is always positive. For bodies vibrating in or close to the water surface the damping, *b*, is caused by the radiation of waves at the motion of the buoy and also by linearized viscous damping through the drag force. The coefficients *a* and *b* are functions of the motion frequency, or wave frequency in waves. See e.g. Figure 4-6 and Figure 4-7 for the sample buoy. *S* is the mooring stiffness and $F(t)$ is the driving force

General mechanics of vibration can be found in some fundamental textbooks e.g. books by Craig[xliii], Roberts and P. D. Spanos[xliv] or Thompson[xlv].

6.2 Free Vibration of a Floating Buoy in Surge

Before the discussion of response to different types of loading we will repeat a little about the free vibrations of the one-degree-of-freedom system. The equation of motion for a buoy in surge can be written

$$(m+a)\ddot{x} + b\dot{x} + Sx = 0 \qquad \text{Equation 6-2}$$

which follows directly from Equation 6-1 setting $F(t) = 0$.

Assuming a solution of the form

$$x = Ce^{\kappa t}, \qquad \text{Equation 6-3}$$

we get the characteristic equation

$$\kappa^2 + 2\xi\omega_N\kappa + \omega_N^2 = 0, \qquad \text{Equation 6-4}$$

where

$\omega_N = \sqrt{S/(m+a)}$ is the "natural" angular frequency, that is, the undamped angular frequency and
$\xi = b/\left(2\sqrt{S(m+a)}\right)$ is the damping factor.

The roots of $\kappa^2 + 2\xi\omega_N\kappa + \omega_N^2 = 0$, Equation 6-4 are

$$\kappa_{1,2} = -\xi\omega_N \pm \omega_N\sqrt{\xi^2 - 1}. \qquad \text{Equation 6-5}$$

These roots are complex, zero or real depending on the value of ξ. The damping factor can thus be used to distinguish between three cases: underdamped ($0 < \xi < 1$), critically damped ($\xi = 1$) and overdamped ($\xi > 1$). See Figure 6-2 for the motion of a body released from the position $x(0) = 1$ m at $t = 0$ s. The underdamped case displays an attenuating oscillation, while the other cases display motions monotonously approaching the equilibrium position. A moored floating buoy in surge would normally display underdamped characteristics with a damping factor of the order of 10^{-3}. Note that an unmoored buoy, $S = 0$ exhibits no surge resonance. The damping factor is often called the damping ratio, as it is equal to the ratio between the current damping coefficient, b, and the critical damping coefficient, $2\sqrt{c(m+a)}$.

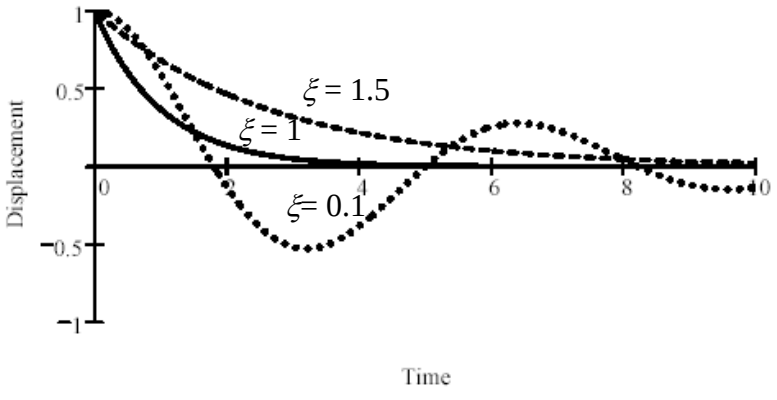

Figure 6-2
Response of a damped SDOF system with various damping ratios.

Table 6-1
Natural frequencies and damping factors for the moored buoy at the two mean offsets.

Mean offset (m)	Stiffness (kN/m)	Natural frequency (s)	Damping factor
6.90	68.0 (Tangential)	10.2	$1.3 \cdot 10^{-3}$
3.89	12.0 (Tangential)	19.9	$0.17 \cdot 10^{-3}0$
	200 (Secant)	6	$75 \cdot 10^{-3}$

The natural frequencies and damping factors for the moored buoy at the two mean offsets are listed in Table 6-1. As the peak period is T_p = 12.9 s and the zero-crossing period is T_z = 10.1 s in the design spectrum, there is a risk of large horizontal resonance motion. In the table there is also a secant modulus listed, which is the mean stiffness for an excursion from 4.5 to 14 m, when the whole chain is lifted.

6.3 Response to Harmonic Loads

A harmonic load

$$F(t) = F_o \cos(\omega t) \qquad \text{Equation 6-6}$$

as from regular waves for instance gives a response of the same harmonic type:

$$x(t) = \hat{x} \cos(\omega t - \varepsilon) . \qquad \text{Equation 6-7}$$

The motion *x(t)* is the stationary response to the harmonic load and is the particular solution to Equation 6-1 with the right hand side *F(t)* given by Equation 6-6.

F_o is the force amplitude
$\omega = 2\pi/T$ the angular frequency
T the time period
$\hat{x}$ the amplitude of the displacement and
ε the phase lag between the force and displacement.

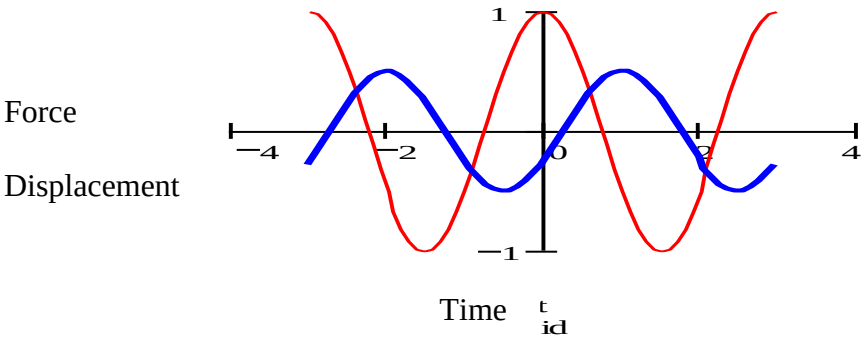

Figure 6-3
The exciting harmonic load *F(t)* and the stationary Response, *x(t)*, for a linear system.

We can solve Equation 6-1 for the given harmonic load, Equation 6-6, simply by substituting the particular solution Equation 6-7 into it. The last equation gives the surge velocity and acceleration of the buoy:

$$x = \hat{x}\cos(\omega t - \varepsilon)$$
$$\dot{x} = -\omega\hat{x}\sin(\omega t - \varepsilon)$$
$$\ddot{x} = -\omega^2\hat{x}\cos(\omega t - \varepsilon)$$

The substitution gives

$$(S - (m+a)\omega^2)\hat{x}\cos(\omega t - \varepsilon) - b\omega\hat{x}\sin(\omega t - \varepsilon) = F_o\cos(\omega t) \qquad \text{Equation 6-8}$$

Using the trigonometric expressions for sine and cosine of angle differences then yields after some manipulation the amplitude $\hat{x}$, which by definition is positive.

$$\hat{x} = \frac{F_o}{\sqrt{\left\{\left(S - (m+a)\omega^2\right)^2 + b^2\omega^2\right\}}} \qquad \text{Equation 6-9}$$

We can solve for the phase angle, ε, also, but this is not of interest in the present context. In Table 6-2 below the amplitude of the excursion around the mean offset is listed for a regular wave with the significant force amplitude $F_o = F_{Msamp}$ = 0.38 MN at T_p or T_z. In the case of a fixed structure the maximum wave would produce the largest force on the structure, however, for the motion of a moored structure, Equation 6-9 gives the asymptotic motion amplitude after many regular force cycles, while the maximum wave just is a transient incident. It may therefore be more appropriate to use the significant wave height, combined with the peak or mean period. Furthermore, we can note that the system is very sensitive to resonance, why we need include drag damping in a time-domain model or at least linearized drag damping to get near realistic results.

Table 6-2
Motion amplitude due to a regular Morison wave force, $F_o = F_{Msamp}$ = 0.38 MN.

Stiffness (kN/m)	Amplitude at f_p (m)	Amplitude at f_z (m)	Mean offset (m)	Combined excursion (m)	
				at f_p	at f_z
200	2.4	2.9	5.4	7.8	8.3
68	15.2	180	6.9	22.1	187
12	12.3	6.5	3.9	16.2	10.4
0	8.8	5.4		8.8	5.4

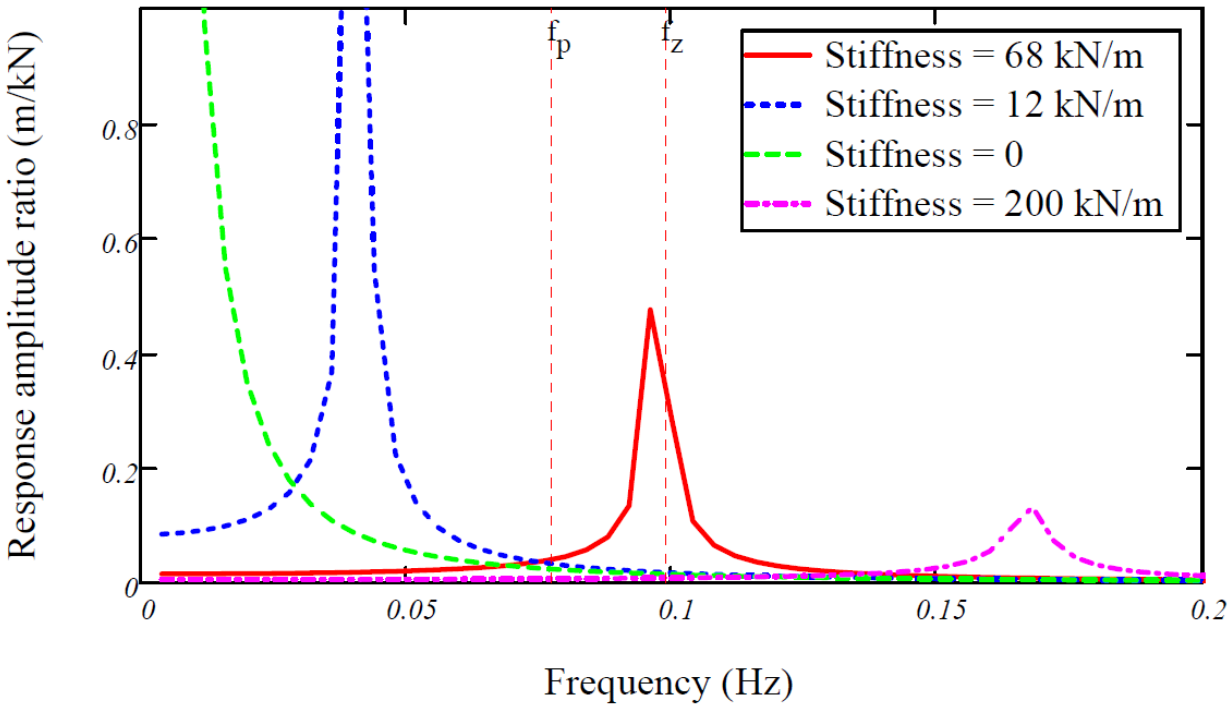

Figure 6-4
The horizontal response amplitude ratio, surge motion amplitude divided by the wave force amplitude, as a function of frequency. The frequencies corresponding to the peak and mean periods are marked to point out the sensitivity to the loading frequency.

6.4 Response Motion in Irregular Waves

6.4.1 Morison mass approach

Using the wave force spectrum based on the Morison mass force approach

$$S_F(f) = \left(f_w(f)\right)^2 S_{PM}(f), \qquad \text{Equation 6-10}$$

we can calculate the surge motion response spectrum as[xxxix]

$$S_x(f) = \frac{S_F(f)}{(S-(m+a)\omega^2)^2+b^2\omega^2} = \frac{\left(f_w(f)\right)^2 S_{PM}(f)}{(S-(m+a)\omega^2)^2+b^2\omega^2} \qquad \text{Equation 6-11}$$

Then the significant motion amplitude can be estimated as

$$x_{1s} = 2\sqrt{m_{0dF}} = 2\sqrt{\sum_i S_x(f_i)\Delta f_i} \qquad \text{Equation 6-12}$$

The result of this calculation is shown in Figure 6-5 and in Table 6-3 below on the lines marked "none" under linearized drag damping. Without consideration of the drag damping the motion becomes unrealistically large as the large horizontal drag damping is not taken into account. It is much larger than the surge radiation damping.

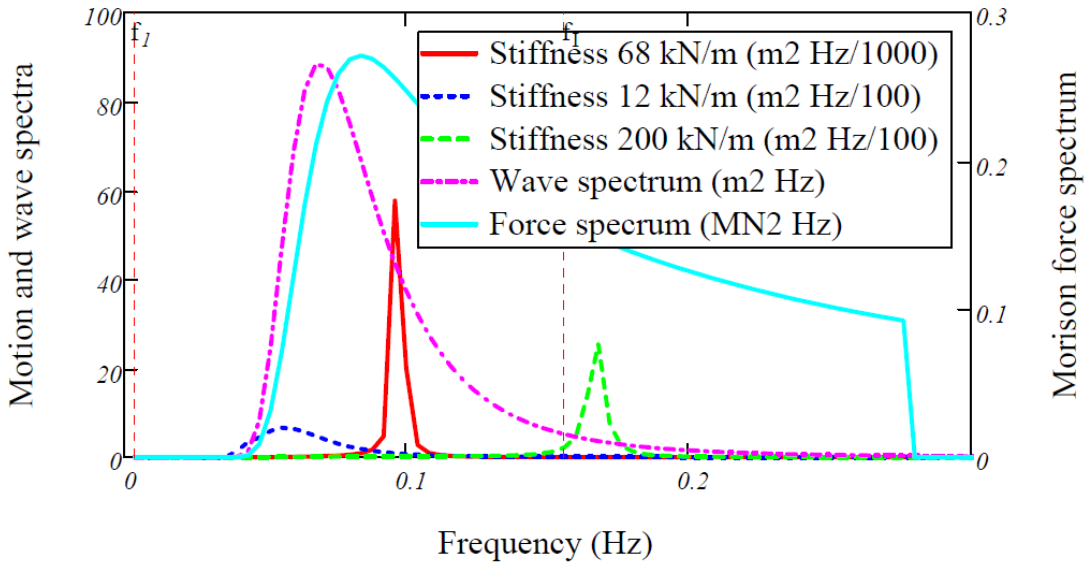

Figure 6-5
Motion spectra, wave spectrum and force spectrum as functions of frequency.
Morison mass approach. No viscous damping.

Table 6-3
Significant linear response in an irregular wave, PM-spectrum, H_s = 8.3 m.

Mean offset (m)		Stiffness (kN/m)	Linearized drag damping	Significant amplitude (m)
5.4	Morison	200	none	7.4
6.9		68	none	37.7
3.9		12	none	7.3
5.4	Diffraction	200	none	3.0
6.9		68	none	31.5
3.9		12	none	9.5
5.4		200	included	2.3
6.9		68	included	5.3
3.9		12	included	5.2

6.4.2 Diffraction force approach

Using the wave force spectrum based on diffraction forces we can similarly form a diffraction-based surge spectrum:

$$S_{dF}(f) = \left(f_{dw}(f)\right)^2 S_{PM}(f), \qquad \text{Equation 6-13}$$

we can calculate the surge motion response spectrum as[xxxix]

$$S_{dx}(f) = \frac{S_{dF}(f)}{(S-(m+a)\omega^2)^2+b^2\omega^2} = \frac{\left(f_{dw}(f)\right)^2 S_{PM}(f)}{(S-(m+a)\omega^2)^2+b^2\omega^2} \qquad \text{Equation 6-14}$$

Then the significant motion amplitude can be estimated as

$$x_{d1s} = 2\sqrt{m_{0dF}} = 2\sqrt{\sum_i S_x(f_i)\Delta f_i} \qquad \text{Equation 6-15}$$

The result of this calculation is shown in Figure 6-6 below and in Table 6-3 above on the lines marked diffraction and "none" under linearized drag damping. Without consideration of the drag damping the motion becomes also here unrealistically large.

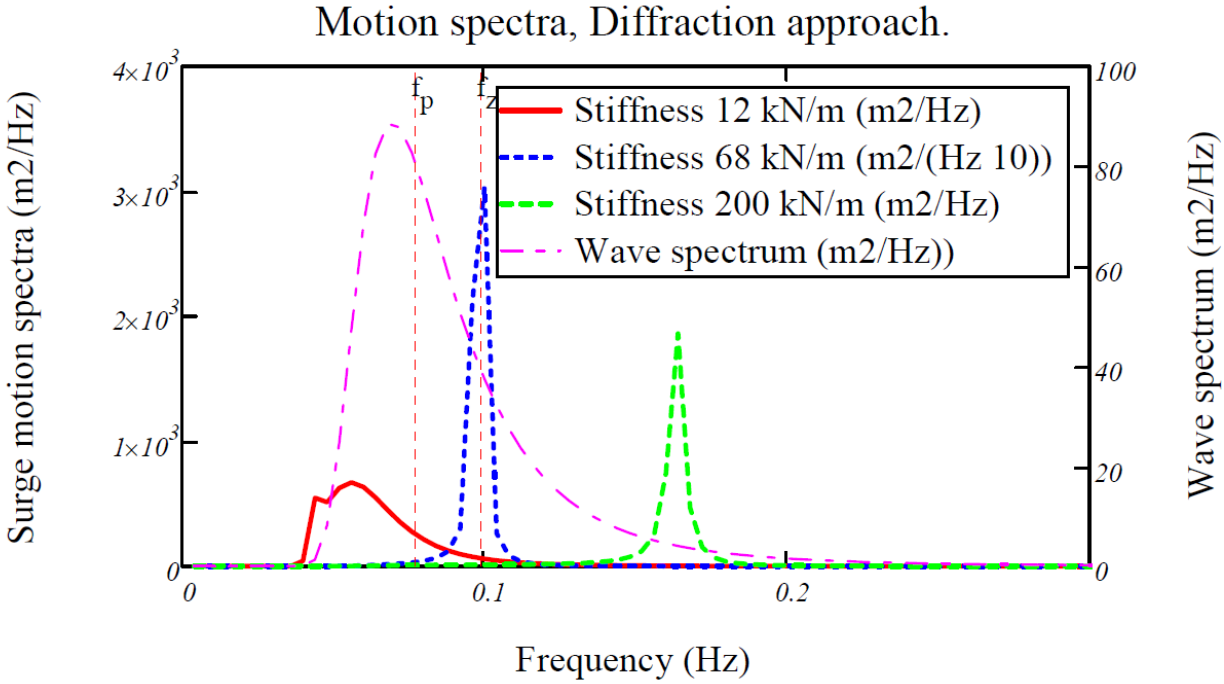

Figure 6-6
Motion spectra and wave spectrum as functions of frequency.
Diffraction approach. No viscous damping.

6.5 Equivalent Linearized Drag Damping

Neglecting the coupling between surge and pitch we can symbolically write the drag damping surge force as

$$F_{D1} = K|u - \dot{x}_1|(u - \dot{x}_1), \qquad \text{Equation 6-16}$$

where K can be set to $(1/2)\rho C_D D h_b$ and u is the undisturbed horizontal velocity of the water in the surge direction and $\dot{x}_1$ the surge velocity of the buoy.

When the non-linear surge damping is important usually $u << \dot{x}_1$ and then we can set

$$F_{D1} = K|\dot{x}_1|(\dot{x}_1), \qquad \text{Equation 6-17}$$

which is simpler but still non-linear.

To assess an equivalent linear coefficient we can compare the dissipated energy over a time, say 3 h, with an equivalent linear expression and the surge velocity

$$x_1(t) = \sum_i(\sqrt{2S_x(f_i)\Delta f_i}\cos(\omega_i t + \varepsilon_i)) \qquad \text{Equation 6-18}$$

Then the dissipated energy can be calculated in two ways

$$\int_0^T K|\dot{x}_1|(\dot{x}_1)^2\,dt = \int_0^T B_{e11}(\dot{x}_1)^2\,dt\,, \qquad \text{Equation 6-19}$$

$$\because B_{e11} = K\frac{\int_0^T |\dot{x}_1|(\dot{x}_1)^2\,dt}{\int_0^T (\dot{x}_1)^2\,dt} \qquad \text{Equation 6-20}$$

That is, the equivalent damping coefficient, B_{e11}, depends on the modulus of the surge motion $|\dot{x}_1|$. The result of this calculation is shown in Table 6-3on the lines marked "included" under linearized drag damping. It should be warned that the specific set of wave components and phase angles used in the numerical realisation affects the equivalent damping and significant amplitudes. In our case we got around 8 m significant amplitude for one realisation and around 5 for another one. However, we may now be able to accommodate the motion. In the figure below there is a comparison between surge response spectra with and without linearized drag damping.

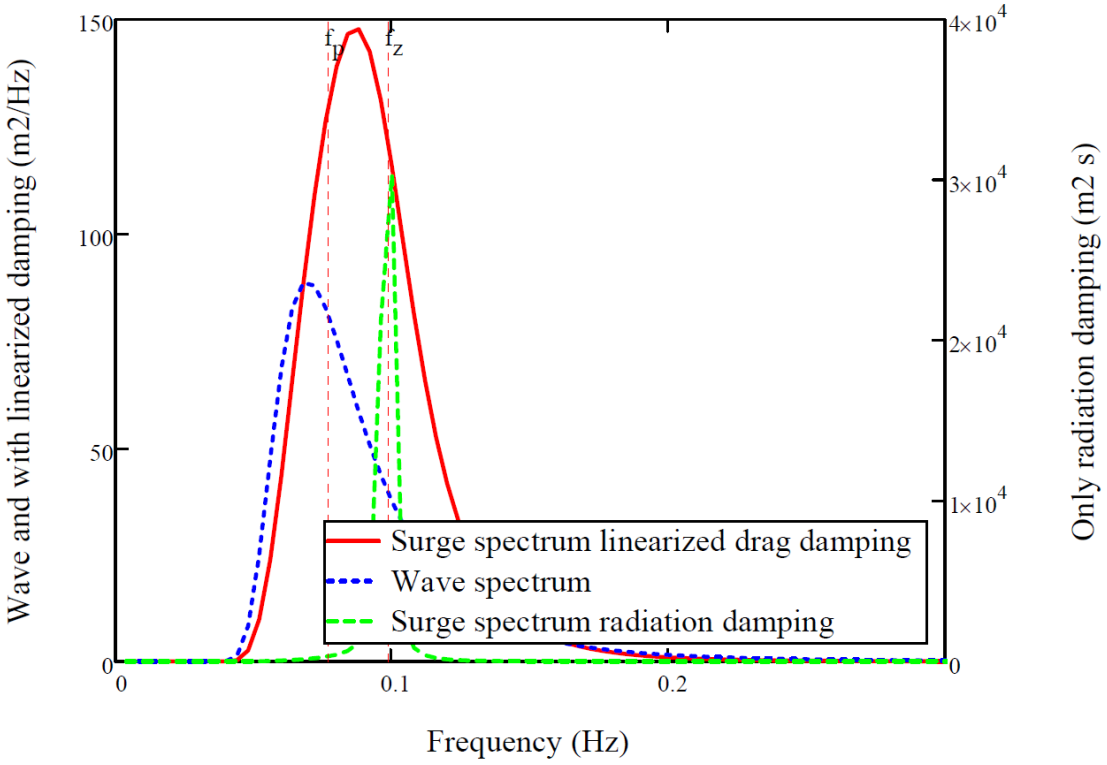

Figure 6-7
Wave spectrum and surge spectra with and without equivalent linearized damping. Note the different vertical scales.

6.6 Second-Order Slowly Varying Motion

In cases where the second-order slowly varying wave force hits the resonance of the moored system, second order slowly varying motion may become large and induce motions of the same order of magnitude as the first-order wave induced motions.

The low-frequency excitation force can be expressed in the frequency-domain by a spectrum (Pinkster, 1975)[xlvi].

$$S_{LF}(\mu) = 8\int_0^\infty S(\omega)\,S(\omega+\mu)C_d\left(\omega+\frac{\mu}{2}\right)\mathrm{d}\omega \qquad \text{Equation 6-21}$$

Here $S(\omega)$ is the wave spectrum and $C_d(\omega)$ is the wave-drift force coefficient. The equation is invoking the Newman[xlvii] approximation and cannot be used if the resonance period is within the wave spectrum periods. Then the full non-linear expression should be used. See e.g. Faltinsen (1990)[xxxiii]. In the present case this is not the case and, anyway, in such cases the motion is dominated by the first-order wave-excited motion.

A sample calculation for this case gives negligible second order slowly varying motion – surge amplitude less than a < mm – compared to the first-order motion. They can be comparable in lower sea states. The reason for negligible second order slowly varying motion is that the resonance period is off the peak of the drift-force spectrum and that the drift force coefficient is small. On the other hand, we should maybe have used the full non-linear expression. However, experience gives that the second-order motions for small objects in high sea states display little second-order motions. See the figure below, where the horizontal resonances at 0.3 and 0.6 rad/s for the two offset tensions pretensions are marked.

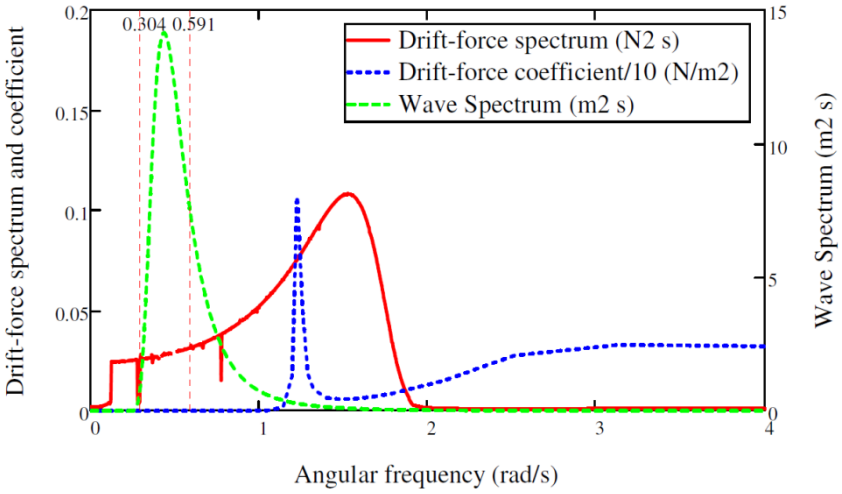

Figure 6-8
Drift-force spectrum, drift-force coefficient and wave spectrum as functions of angular frequency.

6.7 Wave-Drift Damping

In forward speed and in coastal currents the slowly varying motion may be damped by the fact that the encountered wave period and subsequently the wave drift coefficient varies during the slow surge causing a kind of hysteretic damping, called wave-drift damping. As we have negligibly small slowly varying motion in the present case, it is not useful to take this into account.

6.8 Combined Maximum Excursions

Using the design format according to Equation 2-1 we end up with the following table over the design motions X_{C1} and X_{C2}.

$$X_{C1} = X_{mean} + X_{LF\text{-}max} + X_{WF\text{-}sig}$$
$$X_{C2} = X_{mean} + X_{LF\text{-}sig} + X_{WF\text{-}max}$$

Equation 2-1

Table 6-4
Design offsets for quasi-static design. Diffraction results with equivalent drag damping

Stiffness (kN/m)	Mean offset (m)	Wave-frequency amplitude (m)		Low-frequency amplitude (m)		Design offset (m)		Lifted chain length (m) at X_{C2}
		Sign.	Max.	Sign.	Max.	X_{C1}	X_{C2}	
200	4	2.3	4.3			6.3	8.3	219
68	6.5	5.3	9.9	0	0	11.8	16.4	624 (> 509)
12	2.6	5.2	9.7	0	0	7.8	12.3	424

The calculation shows that if we use the secant stiffness modulus and the small modulus (12 kN/m) of the mooring system we fulfil the lifting criterion that the up-wave chain should rest on the bottom close to the anchor: For the stiffer case (68 kN/m) case the chain of the chosen mooring system will lift all the way to the anchor. We would have to modify the mooring system by choosing longer and maybe heavier chains, increasing the number of mooring legs or choosing softer synthetic mooring lines to accommodate the offsets. However, it remains to check the tension requirement

.

7 Required Minimum Breaking Strength

As described in Paragraph 2.2 the calculated tension $T_{QS}(X_C)$ should be multiplied by a partial safety factor $\gamma = 1.7$ for Consequence Class 1 and the product should be less than 0.95 times the minimum breaking strength, S_{mbs}, when statistics of the breaking strength of the component are not available:

$$\gamma T_{QS} < 0.95 S_{mbs} \qquad \text{Equation 2-2}$$

Another usual expression is the utilisation factor

$$u = \frac{\gamma T_{QS}}{0.95 S_{mbs}} < 1 \qquad \text{Equation 2-3}$$

The results of the design calculation is given in Table 7-1. As can be seen only the calculation with the secant modulus S = 200 kN/m meets the requirements. However, this calculation is not according to the standard procedure and may not be accepted. The secant modulus should at least be changed to a value based on the resulting maximum excursion. Solving Equation 2-2 for the minimum breaking strength with T_{QS} = 1.38 MN gives a required minimum breaking strength to 2.5 MN. This corresponds to a chain G3 58 mm[xlviii] with $S_{mbs} = 2.6$ MN and a mass of 77 kg/m[xlix]. A second design loop should be performed with this chain and diffraction methods including linearised damping. If necessary more loops should be performed.

Table 7-1
Comparison between required tension and calculated tension

Stiffness (kN/m)	Design offset (m)		Lifted chain length (m) at X_{C2}	T_{QS} (MN)	γT_{QS} (MN)	$0.95 S_{mbs}$ (MN)	u
	X_{C1}	X_{C2}					
200	6.3	8.3	219	0.37	0.63	1.9	0.33
68	11.8	16.4	624	3.01	5.12	1.9	2.69
12	7.8	12.3	424	1.38	2.35	1.9	1.23

8 Conclusions

The following conclusions can be drawn from the design exercise

- Simplified drag and wind coefficients can be used, because the mean offset is not a dominant part of the total horizontal displacement.
- The Morison wave formulation can be used for objects smaller than a 5^{th} of the wavelength, however with some overdesign. It is important to test various wave frequencies and realistic wave amplitudes. Used in the frequency-domain, skipping the drag component, equivalent linearized drag damping must be added.
- Also using the diffraction method for small objects, equivalent linearized drag damping must be added.
- In the equation of motion, there is a difficulty with progressive stiffening moorings. In the CALM system choosing a stiffness around the mean offset will not give a realistic motion as the stiffness may vary one order of magnitude during the oscillation. It is advised to use time-domain simulations taking at least *S(x)* into consideration, and then the drag damping could as well be introduced as $b(\dot{x}) = CA½\rho|\dot{x}|$.
- In a final design time-domain design tools including mooring dynamics should be used complemented by large scale model tests

9 Acknowledgements

The study is carried out at Dept. of Shipping and Marine Technology, Chalmers, and is co-funded from Region Västra Götaland, Sweden, through the Ocean Energy Centre hosted by Chalmers University of Technology, and the Danish Council for Strategic Research under the Programme Commission on Sustainable Energy and Environment (Contract 09-067257, Structural Design of Wave Energy Devices).

10 References

[i] L. Bergdahl and P. McCullen "Development of a Safety Standard forWave Power Conversion Systems" *Wave Energy Network, CONTRACT N° : ERK5 - CT - 1999-2001*, 2002

[ii] L. Bergdahl and N. Mårtensson "Certification of wave-energy plants – discussion of existing guidelines, especially for mooring design", in *Proceedings of the 2nd European Wave Power Conference,* pp. 114-118 Lisbon, Portugal, 1995

[iii] L. Johanning, G.H. Smith and J. Wolfram, "Towards design standards for WEC moorings", in *Proceedings of the 6th Wave and Tidal Energy Conference*, Glasgow, Scotland, 2005

[iv] Paredes, G., Bergdahl, L., Palm, J., Eskilsson, C. & Pinto, F.: Station keeping design for floating wave energy devices compared to floating offshore oil and gas platforms. *Proceedings of the 10th European Wave and Tidal Energy Conference* 2013

[v] Position Mooring, DNV Offshore Standard DNV-OS-E301, 2013

[vi] *Guidelines on design and operation of wave energy converters*, Det Norske Veritas, 2005 (Carbon Trust Guidelines)

[vii] L.M. Bergdahl and I. Rask, "Dynamic vs. Quasi-Static Design of Catenary Mooring System", 1987 Offshore Technology Conference, OTC 5530

[viii] M.J. Muliawan, Z. Gao and T. Moan, "Analysis of a two-body floating wave energy converter with particular focus on the effect of power take off and mooring systems on energy capture", in OMAE 2011, OMAE2011-49135

[ix] Sesam, MIMOSA, DNV Softwares. [Online]. Available: http://www.dnv.com/services/software/products/sesam/sesamdeepc/mimosa.asp, Visited 2013-03-11

[x] Orcaflex Documentation. [Online]. Available: http://www.orcina.com/SoftwareProducts/OrcaFlex/Documentation/OrcaFlex.pdf, Visited 2013-03-11

[xi] ZENMOOR Mooring Analysis Software for Floating Vessels [Online]. Available: http://www.zentech-usa.com/zentech/pdf/zenmoor.pdf
Visited 2013-03-12

[xii] Sesam SIMO, DNV Softwares. [Online]. Available: http://www.dnv.com/services/software/products/sesam/sesamdeepc/simo.asp, Visited 2013-03-11

[xiii] Sesam, DeepC, DNV Softwares. [Online]. Available: http://www.dnv.com/services/software/products/sesam/sesamdeepc/, Visited 2013-03-11

[xiv] S. Parmeggiano et al. "Comparison of mooring loads in survivability mode of the wave dragon wave energy converter obtained by a numerical model and experimental data", in *OMAE 2012*, OMAE2012-83415

[xv] CASH, In-house program, GVA. [Online]. Available: http://www.gvac.se/engineering-tools/, Visited 2013-03-11

[xvi] Thunder Horse Production and Drilling Unit [Online] Available: http://www.gvac.se/thunder-horse/, Visited 2013-03-11

[xvii] Z. Gao and T. Moan, "Mooring system analysis of multiple wave energy converters in a farm configuration", *Proceedings of the 8th European Wave and Tidal Energy Conference*, Uppsala, Sweden, 2009

[xviii] D.J. Pizer *et al.* Pelamis WEC – Recent advances in the numerical and experimental modelling programme, *Proceedings of the 6th European Wave and Tidal Energy Conference*, Glasgow, UK, 2005

[xix] Q.W. Ma and S. Yan, "QALE-FEM for numerical modelling of nonlinear interaction between 3D moored floating bodies and steep waves,"*Int. J. Numer. Meth. Engng.*, vol. 78, pp. 713-756, 2009

[xx] J. Palm et al CFD Simulation of a Moored FloatingWave Energy Converter, *Proceedings of the 10th European Wave and Tidal Energy Conference*, Aalborg, Denmark, 2013
[xxi] Y. Yu & Y. Li, "Preliminary result of a RANS Simulation for a Floating Point Absorber Wave Energy System under Extreme Wave Conditions", in *30th International Conference on Ocean, Offshore, and Arctic Engineering*, Rotterdam, The Netherlands, June 19-24, 2011
[xxii] Jack/St Malo Deepwater Oil Project [Online]. Available: http://www.offshore-technology.com/projects/jackstmalodeepwaterp/, Visited 2013-03-11
[xxiii] Jack & St Malo Project, "*Response-based analysis*", GVA, KBR, Göteborg, 2010, Internal report
[xxiv] Recommended Practice DNV-RP-C205, October 2013
[xxv] Raphael Waters et al.: Wave climate off the Swedish west coast, *Renewable Energy* 34 (2009) 1600-1606
[xxvi] http://citeseerx.ist.psu.edu/viewdoc/download?doi=10.1.1.135.7884&rep=rep1&type=pdf , visited 2014-05-05.
[xxvii] Peter Söderberg: The Swedish coastal wave climate, *SSPA Report* 104, 1987
[xxviii] *Svensk Lots Del A Allmänna upplysningar*, Sjöfartsverkets Sjökarteavdelning, Norrköping 1992
[xxix] Margheritini, L 2012, *Review on Available Information on Waves in the DanWEC Area*: (DanWEC Vaekstforum 2011). Department of Civil Engineering, Aalborg University, Aalborg. DCE Technical Reports, nr. 135
[xxx] Margheritini, L 2012, *Review on Available Information on Wind, Water Level, Current, Geology and Bathymetry in the DanWEC Area*: (DanWEC Vaekstforum 2011). Department of Civil Engineering, Aalborg University, Aalborg. DCE Technical Reports, nr. 136
[xxxi] Martin Sterndorf: WavePlane, Conceptual Mooring System Design, Sterndorf Engineering, 15 November 2009
[xxxii] A. Pecher, A. Foglia and J.P. Kofoed: Comparison and sensitivity investigations of a CALM and SALM type mooring system for WECs.
[xxxiii] O.M. Faltinsen: *Sea Loads on Ships and Offshore Structures*, Cambridge University Press, 1990.
[xxxiv] Peter Sachs: *Wind Forces in Engineering*, Second Edition, 1978 Elsevier
ISBN: 978-0-08-021299-9
[xxxv] M.R. Haddara, C. Guedes Soares: Wind loads on marine structures, *Marine Structures* 12 (1999) 199-209
[xxxvi] Longuet-Higgins: The mean forces exerted by waves on floating or submerged bodies with application to sand bars and wave-power machines. Proc. R. Soc. London, A352, 462-480 (1977)
[xxxvii] H. Maruo: The drift of a body floating on waves, *J. of Ship Research*, Vol 4, 1960
[xxxviii] Sarpkaya, T. and Isaacson, M.: *Mechanics of Wave Forces on Offshore Structures*, Van Nostrand Reinhold Company, 1981
ISBN 10: 0442254024 / ISBN 13: 9780442254025
[xxxix] Chakrabarti, S.K.: *Handbook of offshore engineering*, Vol. 1, Elsevier, 2005
[xl] R. Yeung, "Added mass and damping of a vertical cylinder in finite-depth waters", *Applied Ocean Research*, ISSN 0141-1187, 1981, Vol.3, No 3, pp. 119 - 133
[xli] Johansson, M.: *Transient motion of large floating structures*, Report Series A:14, Department of Hydraulics, Chalmers University of Technology, 1986
[xlii] A.S. Ramsey: *Statics*, Cambridge, The University Press, 1960
[xliii] Roy R. Craig, Jr.: Structural Dynamics, John Wiley & Sons, New York, 1981
[xliv] J. B. Roberts and P. D. Spanos: Random vibration and statistical linearization, John Wiley & Sons, Chichester, 1990
[xlv] William T. Thompson: Theory of Vibration with Applications, Prentice-Hall Inc., Englewood Cliffs, 1972

[xlvi] J.A. Pinkster: Low-frequency Phenomena Associated with Vessels Moored at Sea. *Society of Petroleum Engineers Journal*, Dec 487-494

[xlvii] J.N. Newman: Second Order Slowly Varying Forces on Vessels in Irregular Waves. *Proc. of International Symposium Dynamics of Marine Vehicles and Structures in Waves*, Ed. R:E:D: Bishop and W:G: Price pp. 182-186. London Mechanical Engineering Publications LTD, 1974

[xlviii] http://www.sotra.net/products/tables/stength-for-studlink-anchor-chain-cables, visited 2014-05-22

[xlix] http://www.sotra.net/products/tables/weight-for-studlink-anchor-chain, visited 2014-05-22